Math. Model. Nat. Phenom. 21 (2026) 16
https://doi.org/10.1051/mmnp/2026010

Mathematical Modelling of Natural Phenomena
www.mmnp-journal.org

CONDITIONAL SUCCESS OF ADAPTIVE THERAPY: THE ROLE OF TREATMENT THRESHOLDS AND NON-EXISTENCE OF OPTIMAL STRATEGIES REVEALED BY MATHEMATICAL MODELLING AND OPTIMAL CONTROL

Lanfei Sun[1,†], Haifeng Zhang[2,†], Kai Kang[1], Xiaoxin Wang[1], Leyi Zhang[1], Yanan Cai[3,4], Lei Zhang[5,*] and Changjing Zhuge[1,*]

Abstract. Adaptive therapy improves cancer treatment by controlling the competition between sensitive and resistant cells through treatment holidays. This study highlights the role of treatment-holidays and the treatment-restarting thresholds in adaptive therapy for tumours composed of drug-sensitive and resistant cells. Using a Lotka–Volterra model, adaptive therapy outcomes are compared with maximum tolerated dose therapy and intermittent therapy outcomes, showing that adaptive therapy success depends critically on the thresholds for pausing and resuming treatment and on competitive interactions between cell populations. Three comparison scenarios between adaptive therapy and other therapies emerge, including uniform-decline where adaptive therapy underperforms regardless of threshold, conditional-improve where efficacy requires threshold optimisation, and uniform-improve where adaptive therapy consistently outperforms alternatives. Tumour initial conditions such as initial burden and initial resistant cell proportion influence outcomes. Threshold adjustments enable adaptive therapy to suppress resistant subclones while preserving sensitive cells, extending progression-free survival. Crucially, this work establishes an optimal control problem for time-to-progression and mathematically proves that under biological constraints like neutral competition or low initial burden, the theoretically optimal strategy is unrealisable as it requires infinitely many treatment holidays, rendering it clinically impractical. These findings emphasize personalised treatment strategies for enhancing long-term therapeutic outcomes.

Mathematics Subject Classification. 92C50, 92C42.

Received February 21, 2025. Accepted March 9, 2026.

Keywords and phrases: Adaptive therapy, treatment-holiday and treatment-restarting threshold, cancer dynamics, mathematical modelling, cell competition.

[1] School of Mathematics Statistics and Mechanics, Beijing University of Technology, Beijing 100124, China.
[2] School of Mathematical Sciences, Jiangsu University, Zhenjiang 212013, China.
[3] College of Science and Engineering, James Cook University, Queensland 4814, Australia.
[4] Western Sydney University, Sydney, Australia.
[5] Department of Liver Surgery, Peking Union Medical College Hospital, Chinese Academy of Medical Sciences & Peking Union Medical College, Beijing 100730, China.

[†] These authors contributed equally to this work.
[*] Corresponding authors: zhanglei44@pumch.cn; zhuge@bjut.edu.cn

1. Introduction

Cancer remains one of the leading causes of death worldwide [1], with its biological complexity and heterogeneity posing significant challenges to conventional therapies such as chemotherapy, radiotherapy, and even immunotherapy [2–4]. Therapeutic resistance, a central obstacle in cancer treatment, arises from the therapeutic selection pressure of pre-existing or induced resistant tumour cells [5–9]. This process drives the evolution of tumour tissue, ultimately leading to the dominance of primary or induced refractory subpopulations, and subsequent relapse and treatment failure [10–12]. The inherent heterogeneity and plasticity of tumour cells often render complete eradication exceedingly difficult, highlighting the necessity of strategies that address the entire tumour population and its evolutionary dynamics, rather than targeting specific subpopulations [3, 13, 14].

Recently, ecological theory has provided an innovative framework for understanding tumour progression, conceptualizing tumours as ecosystems where drug-sensitive and drug-resistant cells compete for resources [15–23]. Within this ecological framework, cancer cells under drug treatment activate regenerative or protective mechanisms to survive near-lethal stress, enabling them to enter a stem cell-like state and transmit resistance to their progeny [24, 25]. This adaptation imposes costs, such as reduced proliferation rates, decreased environmental carrying capacity, and intensified interclonal competition [26, 27].

The conventional maximum tolerated dose (MTD) therapy aggressively eliminates sensitive cell populations. However, this strategy inadvertently disrupts competitive equilibria, allowing resistant subclones to proliferate uncontrollably [21, 28–31]. This unintended consequence of MTD therapy suggests the limitations of conventional eradication-focused paradigms and highlights the need for therapeutic strategies that preserve sensitive cells to maintain ecological suppression of resistant populations [20, 21, 32, 33].

Adaptive therapy (AT) is a dynamic treatment strategy that employs a feedback-controlled approach, adjusting therapeutic intensity and scheduling in response to real-time tumour burden [21, 29, 34]: treatment is paused when tumour burden declines to a certain lower threshold (the treatment-holiday threshold) and resumed upon regrowth to an upper threshold (the treatment-restarting threshold). Adaptive therapy can be classified into dose-skipping (AT-S) and dose-modulating (AT-M) regimens, depending on whether more than two dose rates are used during treatment phases. By retaining a reservoir of sensitive cells, this intermittent dosing modality suppresses resistant subclone expansion and prolongs progression-free survival, as evidenced by clinical successes in prostate cancer and other malignancies.

Despite significant advancements [27, 31, 35–37], further research is needed to refine the optimisation of treatment-holiday and treatment-restarting thresholds, a core parameter governing AT efficacy, as most existing studies focus on the efficiency of adaptive therapy under predefined thresholds. Several studies have explored the effects of varying thresholds on AT outcomes across different scenarios [35, 36, 38–41], providing valuable insights that underscore the importance of threshold adjustments and establishing a solid foundation for further investigation. However, a deeper understanding of the dynamic mechanisms driving context-dependent outcomes under heterogeneous physiological conditions remains essential. It requires a systematic analysis of the underlying dynamical mechanisms by which different thresholds give rise to distinct effects, enhancing conventional empirical threshold selection to achieve an optimal balance between tumour suppression and resistance mitigation. Moreover, it can further facilitate the development of personalized strategies tailored to different conditions. Consequently, quantitative modelling of threshold-driven tumour evolutionary dynamics is essential for advancing precision in adaptive therapy design.

Therefore, this study leverages a mathematical model of tumour evolutionary dynamics to analyse and explain the effects of the thresholds on the outcomes of AT under various conditions of competitive interactions between sensitive and resistant subpopulations, elucidating the biophysical principles underlying threshold-mediated resistance control. The findings are expected to provide theoretical validation for personalized adaptive therapy protocols, facilitating a paradigm shift toward dynamically optimized cancer management.

In summary, this study, as a state-of-the-art work, systematically investigates the impact of treatment-holiday thresholds on adaptive therapy outcomes using a Lotka–Volterra model that simulates the competitive dynamics between drug-sensitive and drug-resistant tumour cell populations. By quantifying the relationship between treatment-holiday threshold and employing time-to-progression (TTP) as an indicator of

progression-free survival, the analysis demonstrates that AT efficacy critically depends on the competition between two subpopulations of cancer cells. Strong competition can allow for the indefinite delay of disease progression, while weak competition requires the benefits of AT. Furthermore, this work also reveals that AT is not uniformly superior to MTD, as its efficiency depends on tumour composition (initial conditions) and patients' personal conditions (parameters). By comparing the TTP between AT and MTD, three distinct scenarios are identified: 1) **uniform-decline**, where AT consistently underperforms MTD regardless of the threshold; 2) **conditional-improve**, where the effectiveness of AT depends on the specific threshold selected; and 3) **uniform-improve**, where AT consistently outperforms MTD. These findings highlight the necessity of precise threshold tuning to optimize treatment outcomes. Collectively, these findings provide a theoretical foundation for refining empirical threshold selection and advancing personalized adaptive therapy protocols, thereby paving the way for dynamically optimized cancer management.

2. Model description

To investigate the effects of different treatment strategies, the tumour dynamics under therapeutic conditions are modelled by the widely used Lotka–Volterra (LV)-type equations [15, 35, 42–46] because the cancer cells behave more similarly to unicellular organisms than to normal human cells [18, 47–49]. The cancer cells are further assumed to be classified into two types: drug-sensitive cells (S), which can be killed by drugs, and drug-resistant cells (R), which cannot be killed by drugs. These two cell types compete within the cancer microenvironment (Fig. 1A), and therefore the LV model is described as the following differential equations (2.1)-(2.3).

$$\frac{\mathrm{d}S}{\mathrm{d}t} = r_S\left(1-\frac{S+\alpha R}{K}\right)\left(1-\gamma\frac{D(t)}{D_0}\right)S - d_S S, \tag{2.1}$$

$$\frac{\mathrm{d}R}{\mathrm{d}t} = r_R\left(1-\frac{\beta S+R}{K}\right)R - d_R R, \tag{2.2}$$

$$N(t) = S(t)+R(t), \tag{2.3}$$

where $D(t)$ denotes the dose curve of therapeutic agents and S and R represent the burdens of the two types of cells respectively. Equation (2.1) describes the growth and death of sensitive cells, which means that in the absence of therapy, their proliferation is regulated by intrinsic rate r_S, logistic competition $\left(1-\frac{S+\alpha R}{K}\right)$ and the death rate is d_S. The drug-dependent suppression of sensitive cells is represented by the factor $\left(1-\gamma\frac{D(t)}{D_0}\right)$ where γ is the killing strength of therapeutic agents on sensitive cells. Although this factor is multiplied with the proliferation terms, it is the integrated effective term taking both suppression of proliferation and increasing death rate for simplicity. Equation (2.2) governs resistant cells, which obey logistic growth $\left(1-\frac{\beta S+R}{K}\right)$ at rate r_R and die at constant rate d_R, unaffected by the drug. K is the carrying capacity of the cancer microenvironment, indicating the maximum number of cells that can be supported.

Moreover, the model equations (2.1)–(2.2) incorporate asymmetric competition between drug-sensitive and drug-resistant cells, characterized by the parameters α and β. Here, α quantifies the inhibitory effect of drug-resistant cells on the growth of sensitive cells, while β represents the impact of drug-sensitive cells on the growth of resistant cells. Specifically, a higher positive value of α implies that resistant cells more strongly reduce the growth potential of sensitive cells, possibly due to resource competition or indirect suppression *via* secreted factors (*e.g.*, growth factors, cytokines). And, a negative value of α indicates that an increase in resistant cells facilitates the growth of sensitive cells, suggesting a commensal or protocooperative relationship between the two sub-populations, rather than mere competition. Similarly, a higher value of β indicates that sensitive cells exert a stronger influence on the growth of resistant cells, potentially through competition for space, nutrients,

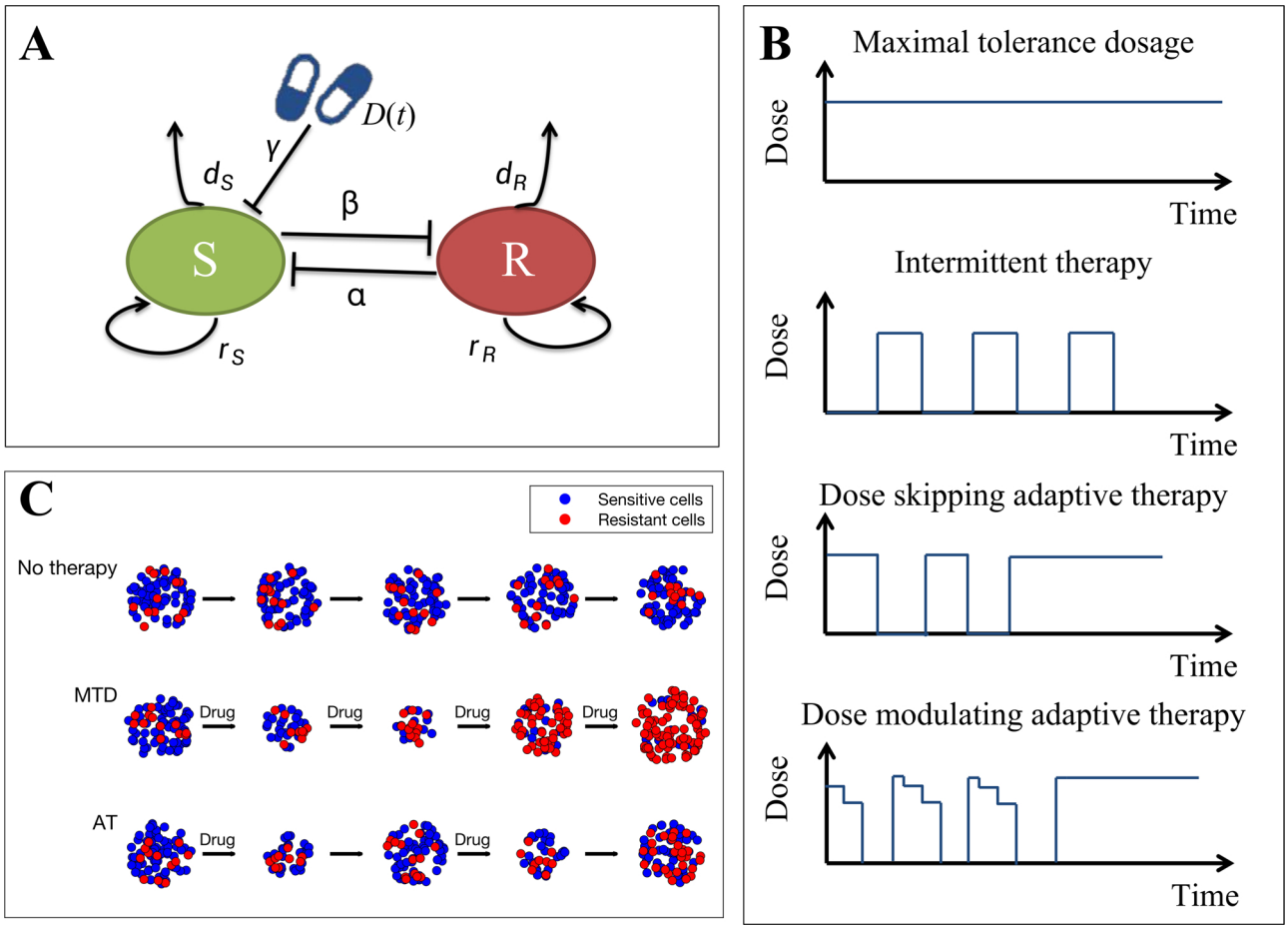

FIGURE 1. Schematic diagram of cancer dynamics models and illustrations of different treatment strategies and their outcomes. **(A)** A schematic representation of the Lotka–Volterra competition between sensitive cancer cells (S) and resistant cancer cells (R). The interactions between these two cell types are influenced by the carrying capacity K and the competition coefficients α and β. Additionally, in the presence of therapeutic agents, sensitive cells are killed by the drugs. **(B)** Schematic illustration of four typical therapeutic strategies: the maximal tolerated dosage (MTD), intermittent therapy (IT), dose-skipping adaptive therapy (AT-S), and dose-modulating adaptive therapy (AT-M). **(C)** Schematic illustration of tumour burden and compositional evolution under distinct therapeutic strategies.

or other resources within the tumour microenvironment while, a negative value of β represents commensalism where sensitive cells promotes the growth of resistant cells.

These competitive interactions determine the dominance relationships between the cell populations. For example, in the absence of therapy, coexistence of the two populations is possible under weak competition (*i.e.*, $\alpha < 1$ and $\beta < 1$), whereas strong competition leads to bistability [15, 35, 50, 51]. Specifically, if the resistant cell population is competitively dominant (*i.e.*, $\alpha > 1$ and $\beta < 1$), the sensitive cell population will eventually become extinct; conversely, if $\alpha < 1$ and $\beta > 1$, the resistant cell population will be eliminated [35]. In addition, the competition coefficients also significantly influence treatment outcomes, with a competitive advantage for sensitive cells being crucial for eradicating resistance [52–54]. Thus, it is necessary to take these competitive dynamics into account in order to design better strategies.

Different therapeutic strategies are characterized by distinct profiles of the dosing function $D(t)$. Two widely used therapeutic approaches and two regimens of adaptive therapy are considered in this work, including maximum tolerated dose, intermittent therapy (IT), dose-skipping adaptive therapy (AT-S) and dose-modulating adaptive therapy (AT-M) (Fig. 1B). The conventional maximum tolerated dose approach seeks to maximize cancer cell eradication by administering the highest dose that a patient can tolerate based on acceptable toxicity levels, which can be defined by continuous administration as (2.4).

$$\text{(MTD)} \qquad D(t) = D_0, \quad \text{for all} \quad t. \tag{2.4}$$

As continuous high-intensity dosage leads to the development of therapeutic resistance through Darwinian selection pressures [29], as well as that high dosage of therapeutic agents causes severe toxicity, the intermittent therapy regimens were proposed, which strategically suspend drug administration during predefined recovery periods and emerged as a clinically utilized strategy for balancing therapeutic efficacy with toxicity management [45]. The IT strategies can be characterized as deterministic treatment cycles as (2.5).

$$\text{(IT)} \qquad D(t) = \begin{cases} D_0, & nT \le t \le nT + T_D, \\ 0, & \text{otherwise.} \end{cases} \tag{2.5}$$

where T is the fixed period of one cycle of treatment, T_D is the duration of drug administration and $n = 1, 2, \cdots$ represents the number of cycles.

As described before, AT dynamically adjusts cancer treatment based on tumour response to prolong efficacy and manage resistance. Two primary approaches within adaptive therapy are dose-skipping and dose-modulating regimens. In dose-skipping adaptive therapy, treatment is administered at the maximum tolerated dose until the tumour burden shrinks to a predetermined threshold (the treatment-holiday threshold C_{TH0}), for example, 50% of the baseline burden; therapy is then paused, allowing the tumour to regrow to antoher upper specific threshold (the treatment-restarting threshold C_{TH1}), usually, 100% of the baseline, before resuming treatment. In dose-modulating adaptive therapy, treatment doses are adjusted at regular intervals based on tumour response: increasing the dose if the tumour grows and decreasing it if the tumour shrinks. This strategy seeks to tailor therapy dynamically to tumour behaviour, potentially reducing toxicity and managing resistance more effectively. Both approaches exploit the competitive dynamics between treatment-sensitive and resistant cancer cells to enhance long-term treatment outcomes and have already succeeded in trials or experiments [29, 31, 37, 55, 56]. Based on the above description, the two AT regimens can be formulated as following equations (2.6) and (2.7) respectively.

$$\text{(AT-S)} \qquad D(t) = \begin{cases} D_0, & \text{if } N(t) \ge C_{\mathrm{TH0}} N_0 \text{ until } N(t) \ge C_{\mathrm{TH1}} N_0, \\ 0, & \text{if } N(t) \le C_{\mathrm{TH1}} N_0 \text{ and } N'(t) > 0 \text{ until } N(t) \ge C_{\mathrm{TH1}} N_0. \end{cases} \tag{2.6}$$

$$\text{(AT-M)} \qquad D(t) = \begin{cases} (1+\delta_1) D_0, & \text{if } N(t) \ge C_{\mathrm{TH2}} N_0, \\ D_0, & \text{if } C_{\mathrm{TH1}} N_0 \le N(t) \le C_{\mathrm{TH2}} N_0 \text{ until } N(t) \le C_{\mathrm{TH1}} N_0, \\ (1-\delta_2) D_0, & \text{if } C_{\mathrm{TH0}} N_0 \le N(t) \le C_{\mathrm{TH1}} N_0 \text{ until } N(t) \le C_{\mathrm{TH0}} N_0. \\ 0, & \text{if } N(t) \le C_{\mathrm{TH2}} N_0 \text{ and } N'(t) > 0 \text{ until } N(t) \ge C_{\mathrm{TH2}} N_0. \end{cases} \tag{2.7}$$

where $N_0 = S_0 + R_0$ is the initial tumour burden and $N'(t)$ is the derivative of $N(t)$ representing whether the tumour burden is growing or shrinking. The dose-modulating thresholds satisfy $C_{\mathrm{TH0}} < C_{\mathrm{TH1}} < C_{\mathrm{TH2}}$ and $C_{\mathrm{TH0}} < 1 < C_{\mathrm{TH2}}$. Notably, the dosing strategies (2.6) and (2.7) represent state-dependent switching mechanisms rather than closed-form mathematical definitions. This implementation induces history-dependent therapeutic decision and consequently, the governing equations (2.1)-(2.3) constitute delay differential equations with history-dependent terms $D(t)$.

TABLE 1. Model parameters and their ranges.

Parameter	Description	Value or range	Reference
K	Total environmental carrying capacity	10000	
α	Competition coefficient of resistant cells on sensitive cells	$(0, +\infty)$	
β	Competition coefficient of sensitive cells on resistant cells	$(0, +\infty)$	
r_S	Proliferation rate of sensitive cells	0.035	[37]
r_R	Proliferation rate of resistant cells	0.027	[37]
d_S	Death rate of sensitive cells	0.0007	[37]
d_R	Death rate of resistant cells	0.00054	[37]
γ	The killing strength of therapeutic agents	1.5	[59]
D_0	Maximal tolerance dose	1	
$n_0 = \frac{N_0}{K}$	Initial tumour burden	$[0, 0.75]$	[58]
$f_R = \frac{R_0}{R_0 + S_0}$	Initial proportion of resistant cells	$[0.001, 0.01]$	[57]
C_{TH0}, C_{TH1}	The treatment-holiday threshold and treatment-restarting thresholds for dose-skipping adaptive therapy		
C_{TH0}, C_{TH1}, C_{TH2}	The dose-modulating thresholds for dose-modulating adaptive therapy		

As a state-of-the-art investigation, this study provides comprehensive parameter analysis rather than case-specific parameter estimation. So, in this work, the parameter values are taken in ranges according to established experimental and clinical studies [35, 37, 57–59]. The proliferation rates of sensitive and resistant cells, *i.e.* r_S and r_R, are derived from *in vitro* experimental data [37], while the drug-induced killing strength γ is sourced from the estimation based on several experiments of cell lines[59]. Given the critical clinical risk associated with large tumour burdens, the initial tumour burden in this study is set as 75% of the environmental carrying capacity [58]. The initial proportion of resistant cells is taken from existing dynamic models [57]. All the baseline parameter values are summarized in Table 1.

3. RESULTS

3.1. The effects of treatment-holiday and treatment-restarting thresholds on the efficiency of adaptive therapy

To investigate the effect of treatment-holiday thresholds on the outcomes of adaptive therapy, a simplified assumption of neutral competition ($\alpha = \beta = 1$) is considered. The outcomes are primarily characterized by the time-to-progression (TTP), which is typically defined as the time at which the tumour burden grows to a certain percentage greater than its initial burden[35, 37, 57–59]. For simplicity, this percentage is set to 120% in this study.

As illustrated in the example of tumour evolution under adaptive therapy (Fig. 2A), during the initial phase of adaptive therapy, drugs are administered to suppress tumour growth primarily through the depletion of sensitive cells. During this stage, the proportion of sensitive cells is high, which aligns with real-world cases. Following the principles of adaptive therapy, treatment is paused when the tumour burden reaches a predefined treatment-holiday threshold $C_{\mathrm{TH0}}N_0$, conventionally set at 50% of the initial tumour burden, *i.e.*, $C_{\mathrm{TH0}} = 0.5$. The treatment holidays allow sensitive cells to repopulate, leading to tumour regrowth. When the tumour burden returns to the treatment-restarting threshold $C_{\mathrm{TH1}}N_0$, treatment resumes, where treatment-restarting threshold is conventionally set at 100% of the initial level N_0, *i.e.*, $C_{\mathrm{TH1}} = 1$. The treatment-holiday threshold C_{TH0} and the treatment-restarting threshold C_{TH1} thus defines a cycle, from the start of treatment to its suspension. These cycles continue until resistant cells dominate the tumour burden, ultimately leading to disease progression.

To further elucidate this phenomenon, phase-plane analysis reveals distinct dynamical regimes with and without treatment (Fig. 2B1-B2). In untreated systems, tumour populations evolve toward coexistence equilibria, as indicated by the nullcline, which mathematically corresponds to the diagonal in Figure 2B1. In the presence of treatment (Fig. 2B2), the long-term steady state shifts to the upper-left corner, where resistant cells dominate the tumour, and sensitive cells eventually disappear. From a dynamical perspective, treatment exerts selective pressure, pushing the tumour toward a resistant cell-dominant state. Therefore, the significance of treatment holidays lies in allowing the tumour to remain longer in a state dominated by sensitive cells, thereby delaying the transition to resistance. In this regard, increasing the treatment-holiday threshold can slow the transition of tumour composition to a resistant state, which implies it is possible to improve adaptive therapy outcomes by modulating the threshold and preventing continuous treatment from driving the tumour toward resistance *via* Darwinian selection [21].

Therefore, the effects of varying the treatment-holiday threshold are examined under different initial tumour states, characterized by the tumour burden (n_0) and the fraction of resistant cells (f_R) (ref. Tab. 1). As shown in Figures 2C1-C3, altering the treatment-holiday threshold significantly impacted TTP. Notably, when the threshold is too low, meaning the tumour never reached the treatment-holiday threshold even during the initial cycle, adaptive therapy lacks treatment holidays and effectively becomes equivalent to MTD therapy. Consequently, as C_{TH0} is around 0, TTP of AT is de facto that of MTD therapy, as shown in the leftmost segments of Figures 2C1-C3.

Importantly, for different initial tumour states, three distinct scenarios emerged when comparing adaptive therapy with MTD. The first scenario, *uniform-decline* (Fig. 2C1), occurs when adaptive therapy consistently performs worse than MTD, regardless of the threshold C_{TH0}. This scenario typically arises in tumours with a low initial tumour burden. The second scenario, *conditional-improve* (Fig. 2C2), occurs when adaptive therapy outperforms MTD only at specific threshold values, suggesting that careful threshold selection is required. The third scenario, *uniform-improve* (Fig. 2C3), occurs when adaptive therapy is always superior to MTD.

The findings highlight the complex relationship between treatment-holiday thresholds and TTP. Moreover, as shown in Figures 2C2-C3, the effect of the threshold is neither monotonic nor continuous, exhibiting discontinuities as the number of treatment cycles changes discretely (Fig. S1). Specifically, in tumours with a low initial burden (Fig. 2C1 and C2), increasing the number of treatment holidays reduces drug exposure, which in turn weakens tumour suppression because under these conditions, the initial tumour burden is low, and therefore, environmental resources remain abundant which makes the changes in the burden of sensitive cells have little impact on the growth rate of resistant cells. In contrast, for tumours with a higher initial burden (Fig. 2C3), where environmental resources are constrained, fluctuations in sensitive cell numbers significantly affect the growth of resistant cells. In such cases, increasing the number of treatment holidays enables sensitive cells to grow and exert stronger suppression on resistant cells, leading to a marked increase in TTP. This aligns with clinical observations in prostate cancer, where intermittent dosing preserved therapeutic sensitivity [37].

To further investigate the impact of initial tumour states on these three scenarios, we examined how different initial tumour burdens and initial resistant cell fractions influence adaptive therapy outcomes (Fig. 2D). When the initial tumour burden exceeds $0.6K$, adaptive therapy uniformly improves TTP, regardless of the initial proportion of resistant cells. However, when the initial tumour burden is below $0.3K$, adaptive therapy can only conditionally improve TTP, implying that careful selection of the treatment-holiday threshold is crucial. In the worst scenario, when the initial tumour burden is very low and the proportion of resistant cells is relatively high (Fig. 2D, top-left), adaptive therapy fails to improve TTP at any threshold, indicating primary resistance. These findings extend prior theoretical work [46] by quantifying phase-transition-like phenomena in threshold-mediated outcomes and verify AT as an ecosystem-inspired therapeutic strategies.

In addition, as the treatment-restarting thresholds C_{TH1} will also influence the duration of treatment holidays, the effects of the treatment-restarting thresholds C_{TH1} are also examined. Simulations with various C_{TH1} reveal a distinct yet analogous pattern in outcomes (Fig. 3). Similar to altering the treatment-holiday threshold, appropriately suspending treatment can also achieve the goal of prolonging TTP, and three different scenarios can be observed as well. The results also indicate, however, that the uniform-improve scenarios are more likely to occur when the proportion of resistant cells is low while with higher proportion of resistant cells, MTD therapy

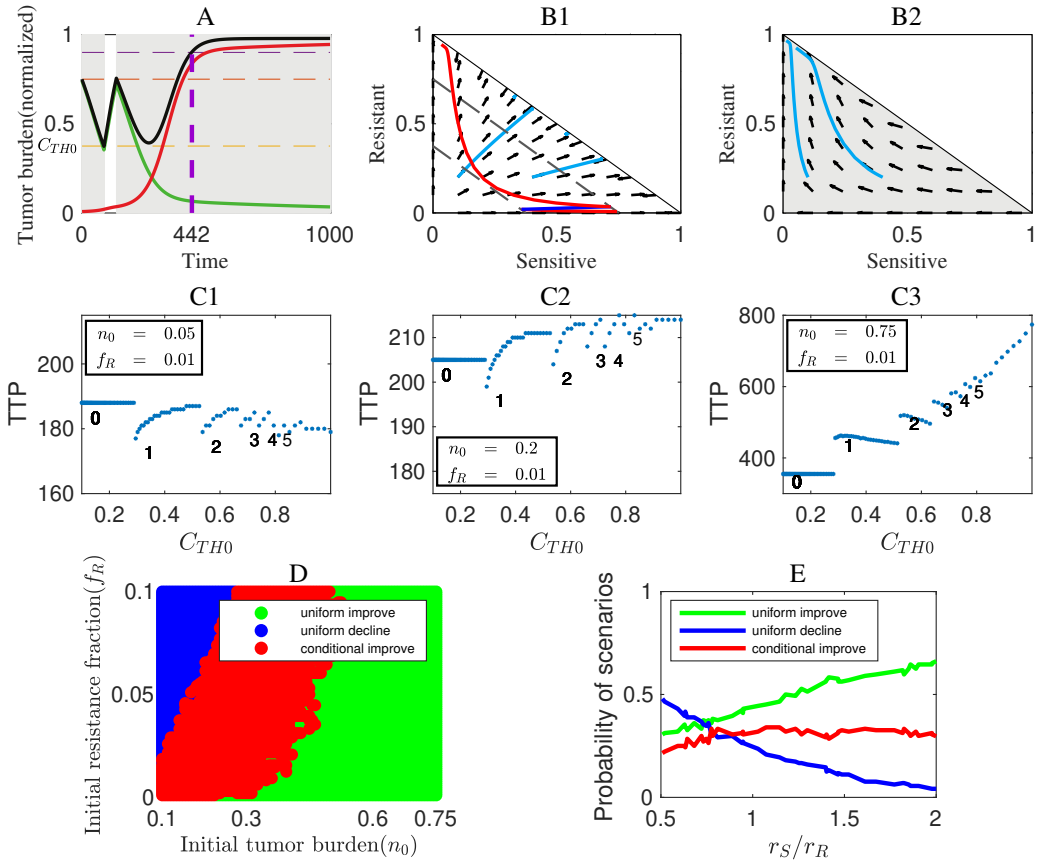

FIGURE 2. Threshold-mediated therapeutic outcomes under neutral competition ($\alpha = \beta = 1$). **(A)** A representative example of tumour evolution under adaptive therapy (AT), where the initial proportion of resistant cells $f_R = 0.01$ and the initial tumour burden as a fraction of carrying capacity is $n_0 = 0.75$. The purple dashed line represents the TTP under the AT strategy with the threshold $C_{\mathrm{TH0}} = 0.5$; the red, green, and black lines represent resistant cells, sensitive cells, and total tumour burden, respectively. Shaded areas indicate periods of active treatment. **(B1-B2)** The phase diagram and the vector field of tumour evolution with and without treatment. Light blue trajectories illustrate the trajectories with different tumour initial states. The upper right blank region represents situations beyond environmental carrying capacity (K). Panel (B1) illustrates the dynamics without treatment, while panel (B2) shows the cases with maximum tolerated dose strategy. The dark blue trajectory in (B1) shows the dynamics of the total tumour burden without treatment, while the red curve illustrates dynamics under AT as shown in panel (A). **(C1)-(C3)** The impact of changing the treatment-holiday threshold on TTPs under different initial tumour compositions. The numbers on the plots indicate the total number of treatment cycles experienced before disease progression, with 0 cycles of AT corresponding to the MTD strategy. Panel (C1) represents a **uniform-decline** scenario of AT, where the TTPs with AT-S are consistently worse than those with MTD; panel (C2) shows a **conditional-improve** scenario, where AT outperforms MTD only for certain threshold values; and panel (C3) demonstrates a **uniform-improve** scenario, where all AT outperforms MTD for all threshold values. **(D)** The dependence of the three scenarios on the initial tumour burden and composition. **(E)** Probability of the three outcome scenarios versus the proliferative fitness ratio r_S/r_R with randomly initial tumour states, demonstrating that a sensitive cell growth advantage ($r_S/r_R > 1$) enhances the AT success probability.

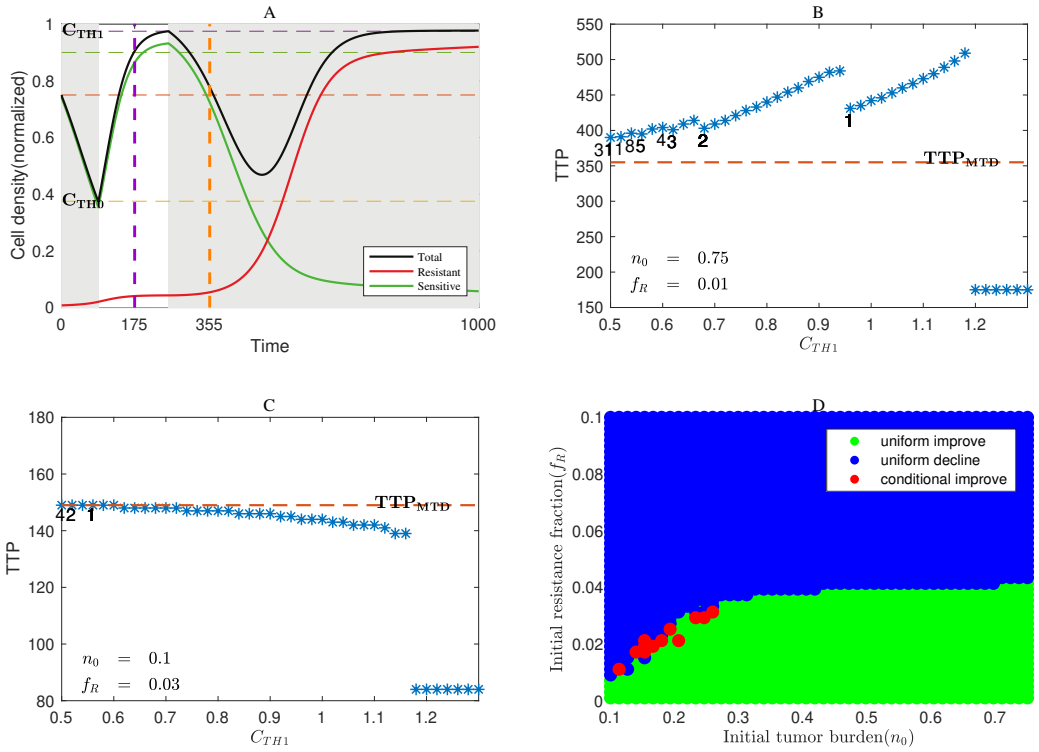

FIGURE 3. The effects of the treatment-restarting threshold on the therapeutic outcomes under neutral competition ($\alpha = \beta = 1$). **(A)** A representative example of tumour evolution under adaptive therapy, where the initial proportion of resistant cells $f_R = 0.01$ and the initial tumour burden as a fraction of carrying capacity is $n_0 = 0.75$. The purple dashed line represents the TTP under the AT strategy with the threshold $C_{\mathrm{TH1}} = 1.3$; the red, green, and black lines represent resistant cells, sensitive cells, and total tumour burden, respectively. Shaded areas indicate periods of active treatment. **(B)-(C)** The impact of changing the treatment-restarting threshold on TTPs under different initial tumour compositions. The numbers on the plots indicate the total number of treatment cycles experienced before disease progression. Panel (B) represents a **uniform-improve** scenario of AT, where the TTPs with AT are consistently better than those with MTD; panel (C) shows a **conditional-improve** scenario, where AT outperforms MTD only for certain threshold values. **(D)** The dependence of the three scenarios on the initial tumour burden and composition.

yields superior results compared to adaptive therapy, regardless of the initial tumour burden (Fig. 3D). It is particularly noteworthy that only a small number of conditionally improved cases are observed here, and as shown in Figure 3C, these few conditionally improved cases are more attributable to computational artifacts rather than reflecting real phenomena. Therefore, in essence, when only the treatment-restarting threshold C_{TH1} varies, there are effectively only two scenarios. This is intuitively reasonable because the advantage of adaptive therapy lies in appropriately suspending treatment to provide a time window for sensitive cells to regrow. The treatment-holiday threshold C_{TH0} determines whether there is an opportunity to suspend treatment, thereby governing the qualitative outcomes of the treatment strategy. In contrast, the treatment-restarting threshold C_{TH1} can only adjust the duration of the treatment suspension, thereby influencing quantitative results. In this sense, adjusting the treatment-holiday threshold is more critical. Furthermore, it should be noted that in Figure 3BC, when C_{TH1} exceeds the upper bound for progression, the TTP becomes very small, which is an issue of definition rather than a characteristic of genuine conditionally improved cases.

Additionally, as both parameters C_{TH0} and C_{TH1} influence the efficacy of adaptive therapy, their combined effects were tested by varying both simultaneously while holding the initial tumour burden and resistant cell fraction constant. Similar to observations with varying C_{TH0} alone, a larger C_{TH1} generally leads to better therapeutic outcomes (Fig. S12). This correlation is attributed to the longer treatment holiday associated with a higher C_{TH1}, which proves beneficial for treatment outcomes. However, a sharp decline in TTP occurs once C_{TH1} exceeds the predefined progression threshold of 1.2, as treatment cannot be restarted before progression is reached when $C_{\mathrm{TH1}} > 1.2$. This result suggests that for patients suitable for AT, administering brief treatment immediately prior to impending progression while maintaining extended treatment holidays can help delay the onset of progression. This also implies that the frequent and controlled cycling between treatment and holiday phases is more beneficial for extending TTP, which will be explored in detail in Section 3.4.

Moreover, clinical implementation faces inherent uncertainty in tumour state assessment and threshold selection, implying that both the treatment-holiday threshold and the initial tumour burden and resistance fraction exhibit random variability. To address this, Monte Carlo simulations were performed to evaluate the probabilities of the three outcome scenarios under parameter variability (Fig. 2E). Inspired by the Norton–Simon Hypothesis [60, 61], which posits that sensitive cells typically have a greater fitness advantage than resistant cells (*i.e.*, sensitive cells have a higher intrinsic proliferation rate than resistant cells), we further explored the effect of the relative growth rate of sensitive cells (r_S/r_R) on the probabilities of the three scenarios. By randomly varying the treatment threshold and, while keeping r_S/r_R fixed, randomly altering r_S and r_R, we found that the probability of the *uniform-improve* scenario increases as the relative fitness of sensitive cells increases. When r_S/r_R is small, adaptive therapy is less likely to improve TTP relative to MTD. Conversely, when r_S/r_R is high, indicating that sensitive cells have a significant growth advantage over resistant cells, adaptive therapy is more likely to enhance TTP. These results confirm that the treatment-holiday threshold has a profound impact on adaptive therapy outcomes and patient-specific tumour characteristics, including initial tumour burden and the relative fitness of sensitive and resistant cells, significantly influence treatment outcomes. These findings align with existing research [27] and demonstrate that r_S/r_R dependence provides quantitative criteria for patient stratification, providing insights for addressing a key challenge in empirical threshold selection [31].

3.2. Context-dependent superiority of adaptive therapy across treatment strategies

This subsection further compares the efficacy of adaptive therapy and intermittent therapy under the uniform-improve scenario, extending the previous comparison with maximum tolerated dose. As indicated in prior results, the effectiveness of different treatment strategies is influenced by treatment parameters. Therefore, to ensure a fair comparison, treatment parameters must be appropriately aligned. A reasonable approach is to compare strategies based on their best achievable outcomes (Fig. 4). Specifically, for intermittent therapy, the optimal treatment cycle and duration should be selected, while for adaptive therapy, the optimal threshold values should be determined.

The optimal parameter combination is determined based on different initial tumour states. Since this study does not focus on identifying these optimal parameters of intermittent therapy, computational details are omitted. However, as previous results suggest that under adaptive therapy in the conditional-improve and uniform-improve scenarios, a threshold closer to 1 generally leads to a longer TTP (Fig. 4). In practical applications, a threshold near 1 would necessitate frequent initiation and cessation of treatment [62], requiring highly precise monitoring of tumour status, which is unrealistic. Similarly, for intermittent therapy, frequent treatment pauses and resumptions are impractical. Given these practical constraints, achieving the true optimal outcome is infeasible. Consequently, only suboptimal treatment outcomes that closely approximate the optimal results are considered as benchmarks for comparison.

For intermittent therapy, the treatment cycle period (T) is examined to range from 7 to 63 time units, with drug administration lasting from 7 to 21 time units (T_D) per cycle. Since this study does not focus on identifying these optimal parameters of IT, computational details are omitted. The result shows that the suboptimal period is $T = 15$ with $T_D = 9$, simulating a regimen in which the patient undergoes both treatment and rest periods within a feasible schedule (Tab. 1 and equations (2.5)). For dose-skipping adaptive therapy,

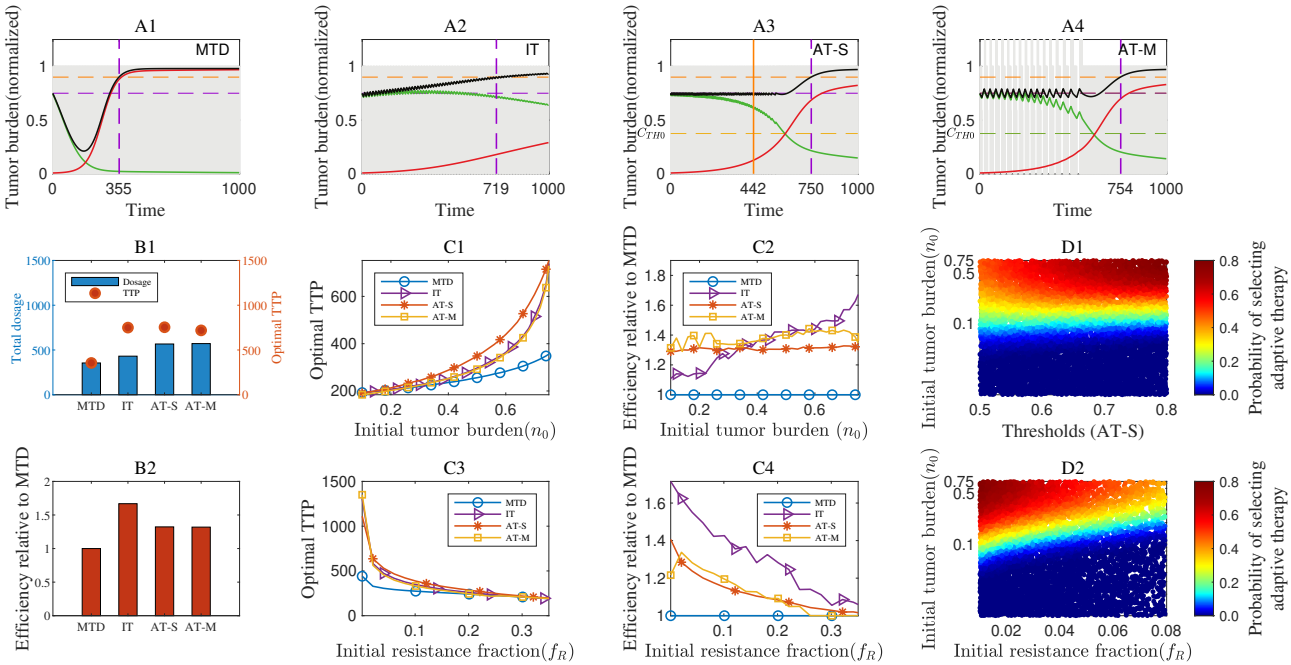

FIGURE 4. Comparison of optimal outcomes under different therapeutic strategies and success landscapes of adaptive therapy. **(A1)-(A4)** tumour evolution dynamics under four therapeutic strategies with optimal treatment-holiday thresholds, given $n_0 = 0.75$ and $f_R = 0.01$. The purple dashed line indicates the TTP with optimal treatment parameters, while the orange solid line in (A2) represents the TTP with the conventional 50% threshold ($C_{\mathrm{TH0}} = 0.5$). Red, green, and black curves represent resistant cells, sensitive cells, and total tumour burden, respectively. Shaded regions denote periods of active treatment. For IT, the treatment interval (T) is 15, and the treatment duration (T_D) is 6. For AT-S, the optimal threshold is close to 1, so here C_{TH0} is set to 0.98. Similarly, for AT-M, the middle threshold is $C_{\mathrm{TH1}} = 1$, and the upper threshold is $C_{\mathrm{TH2}} = 1.05$. **(B1)** Cumulative drug toxicity and the corresponding TTP for the four therapeutic strategies. The cumulative toxicity is quantified by the total drug dosage administered before disease progression, given by equation (3.1). **(B2)** Therapeutic efficiency index, defined as the TTP-to-toxicity ratio as equation (3.1). Here the efficiency indices are displayed as normalized to that of MTD. **(C1)-(C2)** Effects of varying the initial tumour burden on TTP and the efficiency of the four treatment strategies. **(C3)-(C4)** Effects of varying the initial proportion of resistant cells on TTP and the efficiency of the four treatment strategies. **(D1)-(D2)** Success probability landscapes of AT-S as a function of the initial tumour state and treatment threshold. The color at each point represents the probability of AT-S improving treatment outcomes compared to MTD. (D1) illustrates the dependence of success probability on the initial tumour burden and treatment-holiday threshold with randomly varying f_R, r_S, and r_R, which simulates the uncertainty in tumour proliferation and treatment decisions; while (D2) shows its dependence on the initial fraction of resistant cells and initial tumour burden with randomly varying C_{TH0}, r_S, and r_R.

the treatment-holiday threshold is set to $C_{\mathrm{TH0}} = 0.98$, while for dose-modulating adaptive therapy, $C_{\mathrm{TH1}} = 1$ and $C_{\mathrm{TH2}} = 1.05$ are selected as the suboptimal treatment parameters (Fig. 4A1-A4).

In the uniform-improve scenario for adaptive therapy, a comparison of the suboptimal outcomes across the four treatment strategies (Fig. 4A1-A4) reveals that both adaptive therapy strategies result in a longer TTP than intermittent therapy, while intermittent therapy still outperforms MTD. Furthermore, when comparing

the two adaptive therapy strategies, AT-M slightly outperforms AT-S. However, considering the operational complexity of AT-M, AT-S is primarily considered in subsequent discussions to balance efficacy with practical feasibility.

From an efficiency perspective, due to factors such as drug side effects, a higher total drug dosage is not necessarily preferable. Therefore, based on the principle of maximizing TTP with the minimum amount of drug, the contribution of unit dosage to TTP is considered a measure of treatment strategy efficiency (Eq. (3.1), Figure 4B1-B2):

$$\text{Total dosage} = \int_0^{\text{TTP}} D(t)\,\mathrm{d}t, \quad \text{Efficiency} = \frac{\text{TTP}}{\text{Total dosage}} \tag{3.1}$$

It is observed that MTD requires the least total drug dosage (Fig. 4B1), but this is primarily due to its short TTP. Consequently, MTD's efficiency is the lowest among the four treatment strategies (Fig. 4B2). Notably, when efficiency is used as the evaluation criterion, intermittent therapy performs the best (Fig. 4B2). This is because intermittent therapy, compared to adaptive therapy, has longer treatment holidays with a relatively smaller decrease in TTP, resulting in a higher contribution of unit drug dosage to TTP (Fig. 4B2). This suggests that intermittent therapy is a reasonable option, particularly for patients with lower drug tolerance, which is consistent with clinical practice.

Furthermore, to compare the robustness of the four treatments, the stability of TTP and treatment efficiency under uncertainties in patient physiological conditions and tumour status monitoring is examined. The impact of different initial tumour states on TTP and efficiency under the suboptimal parameters for the four strategies is analysed (Fig. 4C1-C4). For different initial tumour burdens, the trends in TTP for the four treatment strategies under the suboptimal parameters are similar; TTP increases with the tumour burden, which is related to the criteria for determining tumour progression. Since progression is determined based on the initial tumour burden, a larger initial tumour burden necessitates a higher burden for progression to occur, leading to this seemingly counterintuitive result (Fig. 4C1). From this perspective, some researchers have proposed a "modifying adaptive therapy" strategy, which delays treatment until the tumour reaches a certain size [63].

Moreover, intermittent therapy shows significant variability with different initial tumour burdens (Fig. 4C2). When the tumour burden is small, intermittent therapy is less efficient than adaptive therapy. As the tumour burden increases, this relationship reverses. Therefore, the robustness of intermittent therapy's efficiency is inferior to that of adaptive therapy. This suggests that when adopting intermittent therapy, a more precise assessment of the patient's specific condition is necessary.

On the other hand, both adaptive therapy strategies and intermittent therapy show similar trends in TTP and efficiency with varying initial proportions of resistant cells (Fig. 4C3-C4), indicating that the optimal TTP is more influenced by cell composition when the proportion of resistant cells is very low. Notably, when the initial proportion of resistant cells is high, the TTP and efficiency of different treatment strategies are close to those of MTD. This is because, when the initial proportion of resistant cells is high, the determining factor for TTP is no longer the competition between sensitive and resistant cells but rather the proliferation of resistant cells themselves, which reduces the differences between treatment strategies.

Furthermore, similar to the previous results, considering the uncertainty in real-world scenarios, the probability of adaptive therapy being the best strategy is explored under conditions of random tumour growth rates and status monitoring. The probability that adaptive therapy results in a longer TTP than both MTD and intermittent therapy is shown in Figure 4D1-D2. In real scenarios, since the tumour growth rate is unknown and tumour composition is difficult to obtain, the dependence of TTP on treatment-holiday thresholds, initial tumour burden, and initial resistant cell proportion is explored under random variations of other factors. Figure 4D1 shows the dependence of the probability of adaptive therapy outperforming other treatment strategies on different thresholds (C_{TH0} and initial tumour burden (n_0), with the other parameters, including the initial resistant cell proportion (f_R) and the intrinsic growth rates of tumour cells (r_S and r_R) varying randomly.

Figure 4D2 shows the dependence of the probability on the initial resistant fraction (f_R) and the initial tumour burden (n_0), with other parameters, C_{TH0}, r_S and r_R, varying randomly.

It can be observed that the probability of selecting adaptive therapy increases significantly when the initial tumour burden is larger. However, when the initial tumour burden is smaller, adaptive therapy does not consistently improve TTP, which aligns with previous findings. Notably, the selection of the treatment-holiday threshold and tumour composition has a weaker impact on the selection of adaptive therapy than the initial tumour burden, indicating that when detailed information about tumour components is unavailable, parameters such as the treatment threshold have less influence, with the initial tumour burden playing a key role. On the other hand, TTP is highly sensitive to the selection of the threshold, among other factors (Figs. 2 and S3-S7). In other words, the selection of the optimal threshold is also dependent on various tumour states. Therefore, when other parameters are randomly varied, the impact of the threshold on TTP becomes overshadowed by fluctuations in these parameters.

These findings are consistent with clinical observations, emphasizing the importance of a precise understanding of tumour dynamics, particularly intrinsic growth rates. If such tumour information is available, treatment strategy selection can be significantly improved, highlighting the critical importance of accurate tumour characterization, especially regarding tumour dynamics.

3.3. Conditional superiority landscapes of adaptive therapy compared to other strategies under non-neutral competition

The competitive interaction between sensitive (S) and resistant (R) cells, governed by coefficients α and β, fundamentally determines tumour evolution dynamics under therapeutic stress [64–67]. Four distinct regimes emerge based on relative competition strengths: 1) weak competition ($\alpha < 1$, $\beta < 1$), 2) strong competition ($\alpha > 1$, $\beta > 1$), 3) asymmetric competition with $\alpha < 1 < \beta$, or 4) $\beta < 1 < \alpha$. It should be noted that cases where $\alpha < 0$ or $\beta < 0$ represent a mutualistic interaction between sensitive and resistant cells. This scenario falls outside the core premise of adaptive therapy, which relies on leveraging competition between cell subpopulations. Consequently, although similar distinct scenarios can be observed under these conditions (Fig. S13), only brief results will be presented at the end of this section and they are not considered in-depth. For the remaining cases, detailed analyses of $\alpha < 1 < \beta$ and $\beta < 1 < \alpha$ cases demonstrate that therapeutic strategies can induce resistant population extinction under specific conditions [35].

In contrast to the case of neutral competition, where progression is inevitable (see Thm. 3.1 in Sect. 3.4), the dynamics differ under strong competition, where untreated tumours evolve toward exclusive dominance of either S or R, depending on initial composition (Fig. 5A), mathematically equivalent to equations (2.1)–(2.3) possessing two stable steady states. Continuous MTD administration drives the tumour toward a stable steady state where sensitive and resistant cells maintain a fixed ratio with unchanged tumour burden (Fig. 5B). In the absence of treatment, the tumour's final state depends on its initial condition, mathematically determined by the basin of attraction in which the system starts. Thus, sensitive cell dominance at initiation leads to resistant cell elimination without treatment, requiring only therapeutic containment to prevent long-term progression. Conversely, initial resistant cell dominance under MTD results in a stable tumour burden with constant cellular proportions. The initial tumour burden determines whether disease progression occurs. Even when exceeding progression thresholds, tumour burden stabilizes below carrying capacity. This property renders the "uniformly-improve" scenario inapplicable for strong competition systems, as therapeutic outcomes primarily depend on initial tumour state rather than threshold calibration (Fig. 5C). That is, as long as the long-term steady state under treatment remains acceptable (Fig. 5B), treatment strategy selection becomes less critical for strong competition cases.

Unlike neutral or strong competition, weak competition ($\alpha < 1$, $\beta < 1$) permits coexistence equilibria regardless of initial states (Fig. 6A), Consequently, the efficacy of adaptive therapy can be inferred directly from the vector field of the dynamical system described by equations (2.1)–(2.3) (Fig. 6AB). However, similar to neutral competition, weak competition also exhibits three distinct therapeutic response scenarios (Fig. 6C),

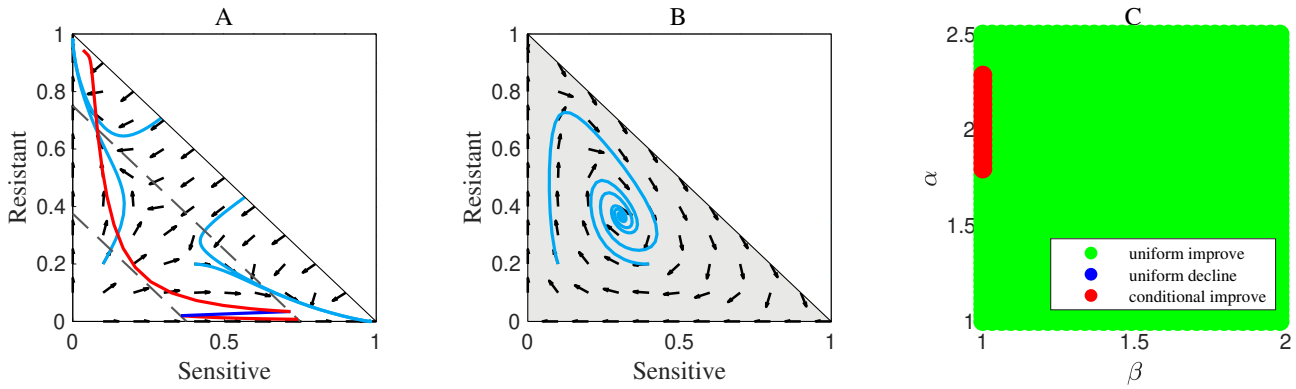

FIGURE 5. **tumour evolution characteristics under strong competition in the presence of therapy. (A)** Phase diagram and vector fields of tumour evolution without treatment. The blue lines indicate that the long-term tumour state depends on the initial conditions. The blank region indicates that the effective tumour burden exceeds the carrying capacity ($S + \alpha R > K$ or $\beta S + R > K$). **(B)** Phase diagram and vector fields of tumour evolution with treatment. The long-term tumour dynamics converge to a state characterized by a heterogeneous composition of sensitive and resistant cells. The other features are similar to those in panel (A). **(C)** The dependence of the three scenarios on the competition coefficients α and β, where, in fact, only two scenarios occur: uniform-decline (red) and conditional-improve (green), with the uniform-improve scenario absent. Here the initial tumour burden is taken as $n_0 = 0.75$ and the fraction of resistant cells is taken as $f_R = 0.01$ with the other parameters as shown in Table 1.

necessitating strategic treatment selection. Given clinical uncertainties, comprehensive parameter-space exploration appears unnecessary and inefficient. The analysis, therefore, focuses on measurable initial tumour burden (n_0) to evaluate adaptive therapy superiority probability under clinical uncertainty, as previous subsections (Fig. 4D1-D2). Less accessible parameters including resistant cell fraction (f_R), thresholds (C_{TH0}), and growth rates (r_S, r_R) are randomized (Fig. 6D0-D8) to simulate the uncertainty in clinical practice. Analysis reveals enhanced adaptive therapy superiority with decreasing α and increasing β (Fig. 6D1-D8), consistent with its premise of leveraging sensitive cells to suppress resistant populations. This relationship weakens when resistant cells evade suppression.

Moreover, it is noted that large initial tumour burdens in strong competition systems reduce the probability of selecting adaptive therapy (Fig. 6 upper-right quadrant) which is significant different from the remaining region. This phenomena results from the bistability that the steady states depend on the initial condition. So the probability of choosing adaptive therapy will be affected by the specific initial condition especially in the condition of strong competition. That is, the force of tumour burden homeostasis may eliminate the effects of the competition by Darwinian selection. It is also worth noting that extended progression timelines may be attributed to the large burdens because of the progression criteria diminishing therapeutic differentiation. So in these cases, surgical intervention may become preferable when tumour burdens approach carrying capacity. Crucially, adaptive therapy selection probability increases with initial tumour burden except at extreme values (Fig. 6D0), paralleling neutral competition observations (Figures 2E and 4D1-D2). These findings confirm the importance of tumour burden as the clinically actionable determinant. And it is also suggesting benefits from precise competition-strength measurements.

Finally, a broad exploration of parameters was conducted to investigate the probability of adaptive therapy providing improvement when α and β are chosen from the interval $(-1, 1)$ (Figs. S13-S14). Accordingly, it is evident that a larger β increases the probability of adaptive therapy improving therapeutic results, owing to the stronger inhibitory effect of sensitive cells on resistant cells (Fig. S14). Meanwhile, TTP increases with a larger

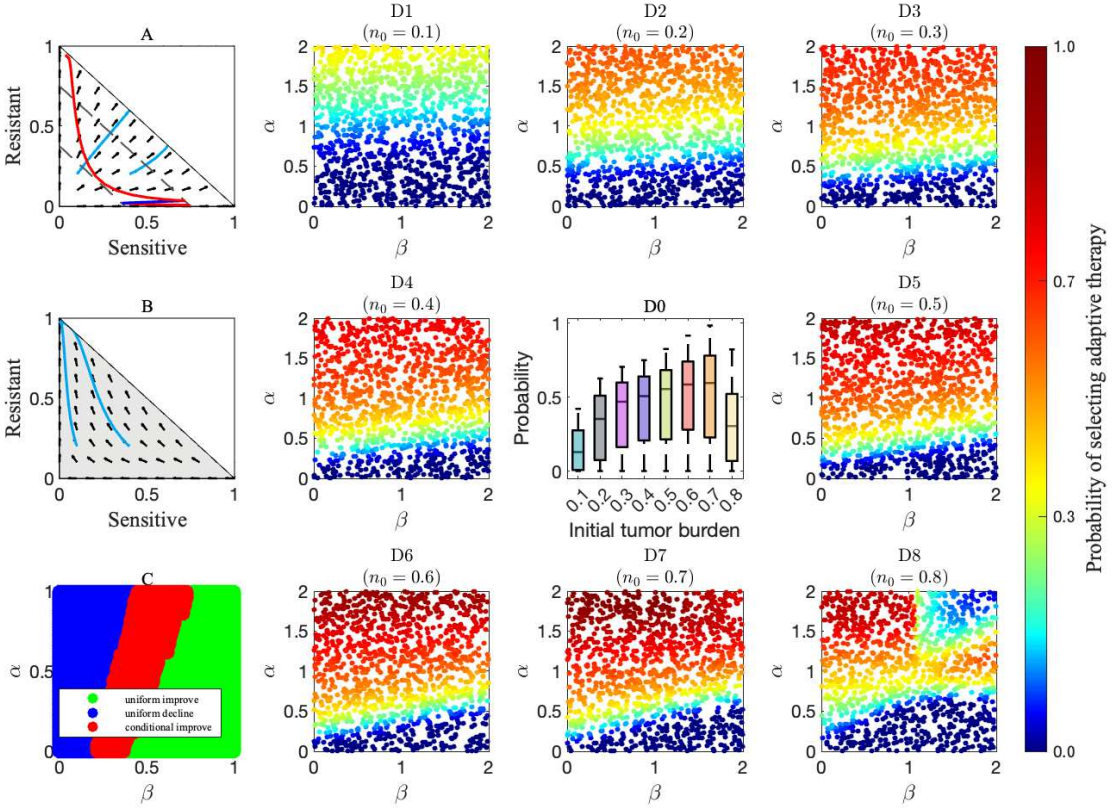

FIGURE 6. Effectiveness of adaptive therapy under conditions of non-neutral competition. **(A)** Phase diagram and vector field of the dynamics of sensitive and resistant cells in the absence of treatment under weak competition. The blank region represents scenarios where the effective tumour burden exceeds the carrying capacity ($S + \alpha R > K$ or $\beta S + R > K$). The blue lines represent tumour evolution trajectories with different initial tumour states. **(B)** Phase diagram and vector field of the dynamics with treatment. The blue lines show that tumour evolution trajectories all move toward a resistant-dominant state. The other elements in the figure are similar to those in panel (A). **(C)** Dependence of the three scenarios on the competition coefficients, with the initial tumour burden $n_0 = 0.75$, the fraction of resistant cells $f_R = 0.01$, and other parameters set as in Table 1. **(D1-D8)** Dependence of the probability of selecting adaptive therapy on competition coefficients, under different initial tumour burdens. Here, the selection of adaptive therapy refers to the condition where the TTP of adaptive therapy is better than that of other strategies. The fraction of resistant cells f_R, cell division rates r_S and r_R, and treatment-holiday thresholds C_{TH0} are randomly sampled to represent various individual conditions. The sample size is 1200 for each pair of competition coefficient values α and β. **(D0)** Overall dependence of the probability of selecting adaptive therapy on the initial tumour burden. Boxplots show the aggregated probabilities calculated from panels (D1)-(D8). **Note** that panels (D0)-(D8) include both weak and strong competition conditions.

initial tumor burden when α and β are randomly selected from $(-1, 1)$ (Fig. S15). It is worth noting that although varying the treatment-holiday threshold can still produce three different scenarios for cases where $\alpha < 0$, only the uniform-decline scenario arises when $\beta < 0$. This is understandable because $\beta < 0$ indicates that sensitive cells promote the growth of resistant cells. Therefore, stopping treatment to allow sensitive cells to regrow cannot possibly suppress the resistant population. Under such conditions, using the maximum tolerated dose to eliminate sensitive cells is the primary strategy for tumor control, making any treatment holiday detrimental

to the outcome. Thus, with $\beta < 0$, the probability of selecting AT is impossible (Fig. S14). In this situation, It is new paradigms other than adaptive therapy utilizing competition that should be proposed.

3.4. The limits and nonexistence of practical optimal therapeutic strategies

As shown in Figure 2C3, TTP is positively correlated with the number of treatment holidays, subject to an upper limit in its computational results. Based on this observation, this subsection provides a theoretical analysis on the limits and optimality of adaptive therapy in terms of calculation of differential equations and optimal control methods.

First, it is proved in Theorem 3.1 that under conditions of neutral competition ($\alpha = \beta = 1$), tumour progression eventually occurs regardless of the therapeutic strategy employed, while similar results for cases of asymmetric competition (both strong and weak) are presented in other literature such as [35, 68, 69]. The proof of Theorem 3.1 is provided at the end of this section.

Theorem 3.1. *Consider the following Lotka–Volterra competition model.*

$$\frac{\mathrm{d}S}{\mathrm{d}t} = r_S\left(1 - \frac{R+S}{K}\right)Sf_1(t) - d_S S f_2(t), \tag{3.2}$$

$$\frac{\mathrm{d}R}{\mathrm{d}t} = r_R\left(1 - \frac{R+S}{K}\right)R - d_R R, \tag{3.3}$$

where $f_1(t)$ and $f_2(t)$ are bounded functions denoting the effecs of treatment. Suppose that the initial condition satisfies $R(0) > 0$, $S(0) > 0$, and $R(0) + S(0) < \dfrac{1}{1+\mu}\left(1 - \dfrac{d_R}{r_R}\right)K$. Then there exists a $T > 0$ such that $R(T) + S(T) > (1+\mu)\,(R(0) + S(0))$.

Secondly, to consider the optimality of adaptive therapy through optimal control theory, it is noted that the primary goal of adaptive therapy is to maximize TTP, and thus it is reasonable to set up the performance index (objective functional) as the maximization of TTP through optimisation of the dose curve $D(t)$, as formalized in equations (3.4)-(3.10) as follows.

$$\sup_{D(\cdot)} J[D(\cdot)] = \int_0^T 1\ \mathrm{d}t = T \tag{3.4}$$

subject to

$$\frac{\mathrm{d}S}{\mathrm{d}t} = r_S\left(1 - \frac{S+\alpha R}{K}\right)\left(1 - \gamma\frac{D(t)}{D_0}\right)S - d_S S, \tag{3.5}$$

$$\frac{\mathrm{d}R}{\mathrm{d}t} = r_R\left(1 - \frac{\beta S + R}{K}\right)R - d_R R, \tag{3.6}$$

$$N(t) = S(t) + R(t), \tag{3.7}$$

$$S(0) = s_0 K,\ R(0) = r_0 K, \tag{3.8}$$

$$N(T) = (1+\mu)n_0 K, \quad \text{where } n_0 = s_0 + r_0, \tag{3.9}$$

$$N(t) < (1+\mu)n_0 K, \quad \text{for } t \in [0, T), \tag{3.10}$$

with parameters satisfying the following constraints (3.11)-(3.14).

$$\alpha, \beta, K, r_S, r_R, d_S, d_R > 0, \tag{3.11}$$

$$\gamma > 1, \quad 0 < \mu \leq 0.5, \tag{3.12}$$

$$0 \leq D_{\min} \leq D(t) \leq D_{\max} \leq D_0, \tag{3.13}$$
$$s_0 + \alpha r_0 < 1, \quad \beta s_0 + r_0 < 1. \tag{3.14}$$

This optimal control problem aims to maximize TTP through an optimized dosing schedule, with tumour growth governed by Lotka–Volterra dynamics. For this formulation, Theorem 3.2 establishes the nonexistence of practically implementable optimal controls under the specified conditions.

Theorem 3.2. *Consider the optimal control problem defined by (3.4)-(3.14), where $D^*(t)$ denotes an optimal control maximizing $J[D(\cdot)]$. Assume that $S'(0) > 0$ and $R'(0) > 0$ when $D(t) \equiv D_{\min} = 0$ and $D^*(t)$ is an optimal control. Then any optimal control $D^*(t)$ maximizing $J[D(\cdot)]$ necessarily has infinitely many points of discontinuity if either of the following conditions is satisfied.*

1. $\alpha = \beta = 1$, *or*
2. $1 \leq \beta \leq \alpha$ *and* $n_0 < \dfrac{1}{(1+\mu)(1+\beta)}$.

The conditions $S'(0) > 0$ and $R'(0) > 0$ under $D(t) \equiv D_{\min} = 0$ are biologically reasonable, as they indicate that the tumour burden remains below the microenvironment's carrying capacity, enabling tumour growth in the absence of therapy. Furthermore, Theorem 3.2 combined with Pontryagin's Maximum Principle implies that any optimal control (if it exists) must undergo infinitely many switches between maximum and minimum dosing levels, rendering it clinically impractical.

Theorem 3.2 states that when competition is neutral, or when resistant cells outcompete sensitive cells with lower initial tumour burden, there is no clinically feasible optimal treatment protocol.

Before proving the theorem, some typical calculations for the optimal control problem and lemmas are needed. Firstly, the necessary condition for the optimal control problem should be calculated using Pontryagin's Maximum Principle. The Hamiltonian $\mathcal{H}$ is defined as equation (3.15).

$$\begin{aligned}\mathcal{H}(S,R,\lambda_S,\lambda_R,D) &= 1 + \lambda_S \frac{\mathrm{d}S}{\mathrm{d}t} + \lambda_R \frac{\mathrm{d}R}{\mathrm{d}t}. \\ &= 1 + \lambda_S \left[r_S \left(1 - \frac{S+\alpha R}{K}\right)\left(1 - \gamma \frac{D}{D_0}\right) S - d_S S \right] + \lambda_R \left[r_R \left(1 - \frac{\beta S + R}{K}\right) R - d_R R \right].\end{aligned} \tag{3.15}$$

Thus, the equations for the costates are given as following equations (3.16) and (3.17).

$$\begin{aligned}\frac{\mathrm{d}\lambda_S}{\mathrm{d}t} &= -\frac{\partial \mathcal{H}}{\partial S} \\ &= \lambda_S \left[d_S - r_S \left(1 - \frac{2S + \alpha R}{K}\right)\left(1 - \gamma \frac{D(t)}{D_0}\right)\right] + \lambda_R r_R \frac{\beta R}{K}\end{aligned} \tag{3.16}$$

$$\begin{aligned}\frac{\mathrm{d}\lambda_R}{\mathrm{d}t} &= -\frac{\partial \mathcal{H}}{\partial R}, \\ &= \lambda_S r_S \frac{\alpha S}{K}\left(1 - \gamma \frac{D(t)}{D_0}\right) + \lambda_R \left[d_R - r_R \left(1 - \frac{\beta S + 2R}{K}\right)\right].\end{aligned} \tag{3.17}$$

with the transversality conditions as boundary conditions (equations (3.18)-(3.20)).

$$\lambda_S(T) = \nu, \tag{3.18}$$
$$\lambda_R(T) = \nu, \tag{3.19}$$

where ν is the Lagrange multiplier associated with the terminal constraint $N(T) = (1+\mu)n_0K$, obtained from the terminal condition of the Hamiltonian as given by equation (3.20).

$$\mathcal{H}(S(T), R(T), \lambda_S(T), \lambda_R(T), D(T)) = 0.$$

So the ν should satisfies the equation

$$\mathcal{H}(S(T), R(T), \nu, \nu, D(T)) = 0. \tag{3.20}$$

According to Pontryagin's Maximum Principle, since the Hamiltonian $\mathcal{H}$ is linear in $D(t)$ (Eq. (3.15) and $D^*(t)$ subjects to (3.13), hence, $D^*(t)$ is determined by the sign of the switching function $\Phi(t)$ given by the equation (3.21).

$$D^*(t) = \begin{cases} D_{\max}, & \text{if } \Phi(t) > 0, \\ D_{\min}, & \text{if } \Phi(t) < 0, \\ \text{singular}, & \text{if } \Phi(t) = 0 \text{ on } [t_1, t_2], \end{cases} \tag{3.21}$$

where

$$\Phi(t) = -\lambda_S(t) \cdot r_S \left(1 - \frac{S(t) + \alpha R(t)}{K}\right) \gamma \frac{S(t)}{D_0}. \tag{3.22}$$

In summary, the equations for the optimal solution $D^*(t)$ of the optimal control problem (if it exists) are summarized in the following Lemma 3.3.

Lemma 3.3. *If the optimal control problem* (3.4)-(3.14) *has a solution with optimal control* $D^*(t)$*, then* $D^*(t)$ *satisfies the following equations:*

$$\frac{\mathrm{d}S}{\mathrm{d}t} = r_S \left(1 - \frac{S + \alpha R}{K}\right) \left(1 - \gamma \frac{D^*(t)}{D_0}\right) S - d_S S, \tag{3.23}$$

$$\frac{\mathrm{d}R}{\mathrm{d}t} = r_R \left(1 - \frac{\beta S + R}{K}\right) R - d_R R, \tag{3.24}$$

$$\frac{\mathrm{d}\lambda_S}{\mathrm{d}t} = \lambda_S \left[d_S - r_S \left(1 - \frac{2S + \alpha R}{K}\right) \left(1 - \gamma \frac{D^*(t)}{D_0}\right)\right] + \lambda_R r_R \frac{\beta R}{K}, \tag{3.25}$$

$$\frac{\mathrm{d}\lambda_R}{\mathrm{d}t} = \lambda_S r_S \frac{\alpha S}{K} \left(1 - \gamma \frac{^*(t)}{D_0}\right) + \lambda_R \left[d_R - r_R \left(1 - \frac{\beta S + 2R}{K}\right)\right], \tag{3.26}$$

$$N(t) = S(t) + R(t), \tag{3.27}$$

$$S(0) = s_0 K, \;\; R(0) = r_0 K, \tag{3.28}$$

$$N(T) = (1+\mu)n_0 K, \quad \textit{where } n_0 = s_0 + r_0, \tag{3.29}$$

$$N(t) < (1+\mu)n_0 K, \quad \textit{for } t \in [0, T), \tag{3.30}$$

$$\lambda_S(T) = \nu, \tag{3.31}$$

$$\lambda_R(T) = \nu, \tag{3.32}$$

$$\mathcal{H}(S(T), R(T), \nu, \nu, D^*(T)) = 0, \tag{3.33}$$

$$\Phi(t) = -\lambda_S(t) \cdot r_S \left(1 - \frac{S(t) + \alpha R(t)}{K}\right) \gamma \frac{S(t)}{D_0}, \tag{3.34}$$

$$D^*(t) = \begin{cases} D_{\max}, & \text{if } \Phi(t) > 0, \\ D_{\min}, & \text{if } \Phi(t) < 0, \\ \textit{singular}, & \text{if } \Phi(t) = 0 \text{ on } [t_1, t_2]. \end{cases} \tag{3.35}$$

The Lemma 3.3 also provides a numerical method based on a forward-backward sweep scheme if the optimal control exists.

For simplicity and considering biological realism, hereafter in this section, we make the following assumptions (3.36)–(3.37).

$$D_{\min} = 0,\ 1 - \gamma\frac{D_{\max}}{D_0} < 0, \tag{3.36}$$

and

$$S(0),\ R(0),\ S'(0),\ R'(0) > 0 \text{ when } D(t) \equiv D_{\min} = 0. \tag{3.37}$$

Biologically, these assumptions indicate that the tumour burden is within the carrying capacity of the microenvironment, enabling tumour growth.

In addition, to simplify notation, the following symbols are introduced throughout this Sect. 1) let $\bar{D} = -\left(1 - \gamma\frac{D_{\max}}{D_0}\right) > 0$ denote the factor in (3.5). 2) let $S^*(t),\ R^*(t), N^*(t) = S^*(t) + R^*(t)$ be the state solution for the optimal control problem (3.4)-(3.14). And 3) let T^*be the optimal terminal time (objective value), *i.e.*, the time point such that $N^*(T^*) = (1+\mu)n_0K$ if the optimal control exists.

Based on the necessary condition, more properties of the optimal control $D^*(t)$ can be obtained as Lemma 3.4-3.6.

Lemma 3.4. *Under the condition of Theorem 3.2, if there exists an optimal control for the optimal control problem (3.5)-(3.14), the costate corresponding to the S variable must be negative at the terminal point T^*, $\lambda_S(T^*)$ must be negative and the derivative $\left.\frac{\mathrm{d}N^*}{\mathrm{d}t}\right|_{t=T^*}$ must be positive.*

Proof. Under the condition of $D(t) \equiv D_{\min} = 0$, it is straightforward to verify that $S'(t) > 0$ and $R'(t) > 0$ for all $t \in [0, T]$ except possibly at isolated points if $S'(0) > 0$ and $R'(0) > 0$ using a standard argument for ordinary differential equations by contradiction as follows. First, for the case that $S'(t) = R'(t) = 0$ it will reach a contradiction by the uniqueness theorem of ordinary differential equations, as the constant solution is also a solution. For the case that $S'(t) = 0$ while $R'(t) > 0$ (without loss of generality). Assume that $t' = \inf\{t > 0 | S'(t) \le 0\}$ and $t'' = \inf\{t > 0 | R'(t) \le 0\}$, then because $S(t)$ and $R(t)$ is continuously differentiable and $S'(0) > 0,\ R'(0) > 0$, we have $t' > 0,\ t'' > 0$. So without loss of generality, we can assume that $t' < t''$. In this case, $S'(t') = 0$ and $S'(t) > 0, R'(t) > 0$ for $t < t'$. And thus, $R'(t') > 0$ in some semi-neighbourhood of t', $t \in (t', t' + \delta')$. So, it is impossible that $S'(t) = 0$ on any neighbourhood of t' because the right-hand side of (3.5) cannot keep zero when $R'(t) > 0$ under the assumption that $S(t) \neq 0$.

According to (3.21), as $S'(t) > 0$ without drugs ($D(t) \equiv 0$), it follows that

$$\left(1 - \frac{S(t) + \alpha R(t)}{K}\right) > \frac{d_S}{r_S} S(t) > 0.$$

So it is impossible that the case $\Phi(t) \equiv 0$ on some interval happens. Thus, the optimal control (if it exists) can be written as (3.38) as follows.

$$D^*(t) = \begin{cases} D_{\max}, & \text{if } \lambda_S(t) < 0 \\ D_{\min}, & \text{if } \lambda_S(t) > 0. \end{cases} \tag{3.38}$$

Therefore, by (3.18)-(3.20), the boundary value of the costate $\lambda_S(t)$ must satisfy

$$\lambda_S(T^*) = -\frac{1}{\left.\frac{\mathrm{dN}^*}{\mathrm{d}t}\right|_{t=T^*}} < 0. \tag{3.39}$$

And this completes the proof. □

The Lemma 3.4 is consistent with the fact that at the time of progression, the total tumour burden is growing and progression always occurs during drug administration. Otherwise, intuitively, drug administration can always slow down the growth of tumour within a small time interval as sensitive cells are being eliminated.

Lemma 3.5. *Assume the optimal control problem has a solution that is piecewise constant with finitely many discontinuities. If $\alpha = \beta = 1$, there exists $T_0 < T^*$ such that $r_R R^*(t) > \bar{D} r_S S^*(t)$ holds for every $t \in [T_0, T^*]$.*

Proof. For simplicity, the asterisk in the superscript are omitted in this proof. According to Lemma 3.4, in some neighbourhood of T^*, the following holds.

$$\begin{aligned} \frac{\mathrm{d}N}{\mathrm{d}t} &= -r_S \left(1 - \frac{S+R}{K}\right) \bar{D} S - d_S S + r_R \left(1 - \frac{S+R}{K}\right) R - d_R R \\ &= \left(1 - \frac{S+R}{K}\right) (-r_S \bar{D} S + r_R R) - d_S S - d_R R > 0. \end{aligned} \tag{3.40}$$

So $\left(1 - \frac{S+R}{K}\right) (-r_S \bar{D} S + r_R R) > d_S S + d_R R > 0$ and therefore

$$r_R R(t) > \bar{D} r_S S(t), \quad \text{for } t \in [T_0, T^*]. \tag{3.41}$$

□

Lemma 3.6. *Assume that $1 \le \beta \le \alpha$ and $S(0) + R(0) < \frac{K}{(1+\mu)(1+\beta)}$. If the optimal control problems (3.4)-(3.14) has a piecewise constant optimal control according to PMP, there exists $T_0' < T^*$ such that $r_R \beta R^*(t) > \bar{D} r_S S^*(t)$ for every $t \in [T_0', T^*]$.*

Proof. Similar to the proof of Lemma 3.5, the asterisks are also omitted in this proof. And, in a neighbourhood of T^*, the following holds.

$$\frac{\mathrm{d}N}{\mathrm{d}t} = r_S \left(1 - \frac{S+\alpha R}{K}\right) (-\bar{D})\, S - d_S S + r_R \left(1 - \frac{\beta S + R}{K}\right) R - d_R R > 0. \tag{3.42}$$

And thus,

$$\left(1 - \frac{S+\alpha R}{K}\right) (-\bar{D} r_S S + r_R \beta R) + r_R R \left(\frac{(\beta-\alpha)S}{K} + (1-\beta)\frac{K - (\beta+1)R}{K}\right) - d_S s - d_R R > 0, \tag{3.43}$$

Moreover, since $n_0K = S(0) + R(0) < \dfrac{K}{(1+\mu)(1+\beta)}$, the threshold of progression is thus $(1+\mu)n_0K < \dfrac{K}{1+\beta}$. So the final state of $R(t)$ should satisfies $S(T^*) < N(T^*) < \dfrac{K}{1+\beta}$. Therefore, $\dfrac{(\beta-\alpha)S}{K} + (1-\beta)\dfrac{K-(\beta+1)R}{K} < 0$. Also because that $1 < \beta < \alpha$, so we have that $-\bar{D}r_SS + r_R\beta R > 0$ which, according to the simplification of the notations, implies that $r_R\beta R^*(T^*) > \bar{D}r_SS^*(T^*)$.

And the result of the lemma is followed by a common argument of calculus. □

Now the lemmas are sufficient to prove the main Theorem 3.2.

Proof of Theorem 3.2. By contradiction, assume the optimal control $D^*(t)$ has only finitely many discontinuities. Then, by Pontryagin's Maximum Principle (PMP), $D^*(t)$ is a piecewise constant function whose range has only two values. Let T_1 denote the last discontinuity point of the optimal control. So we have that $D^*(t) = D_{\max}$ for $t \in [T_1, T^*]$ and moreover, from Lemma 3.5 and Lemma 3.6, we can choose $T_2 \in [T_1, T^*)$ such that $N'(t) > 0$ and $r_R\beta R(t) > \bar{D}r_SS(t)$ hold for all $t \in [T_2, T^*]$.

Now we are going to prove that there exists $\Delta t > 0$ such that the state solution has a better termination time than T^* with $D_{\Delta t}(t)$ defined as the following (3.44).

$$D_{\Delta t}(t) = \begin{cases} D_{\min}, & t \in [T^* - 2\Delta t, T^* - \Delta t], \\ D^*(t), & \text{otherwise.} \end{cases} \tag{3.44}$$

Let $S_{\Delta t}(t)$, $R_{\Delta t}(t)$, $N_{\Delta t}(t) = S_{\Delta t}(t) + R_{\Delta t}(t)$ denote the solution with this $D_{\Delta t}(t)$. Then $N^*(t)$ and $N_{\Delta t}(t)$ obey the same differential equations for all t except $t \in [T^* - 2\Delta t, T^* - \Delta t]$.

Moreover, by denoting $t_i = T^* - (2-i)\Delta t$, $i = 0, 1, 2$ and $S_0^* = S^*(t_0)$, $R_0^* = R^*(t_0)$, then we have equations (3.45)-(3.52).

$$S^*(t_1) = S_0^* + \left[r_S\left(1 - \frac{S_0^* + \alpha R_0^*}{K}\right)(-\bar{D})S_0^* - d_SS_0^*\right]\Delta t + o(\Delta t), \tag{3.45}$$

$$R^*(t_1) = R_0^* + \left[r_R\left(1 - \frac{\beta S_0^* + R_0^*}{K}\right)R_0^* - d_RR_0^*\right]\Delta t + o(\Delta t), \tag{3.46}$$

$$S^*(t_2) = S^*(t_1) + \left[r_S\left(1 - \frac{S^*(t_1) + \alpha R^*(t_1)}{K}\right)(-\bar{D})S^*(t_1) - d_SS^*(t_1)\right]\Delta t + o(\Delta t), \tag{3.47}$$

$$R^*(t_2) = R^*(t_1) + \left[r_R\left(1 - \frac{\beta S^*(t_1) + R^*(t_1)}{K}\right)R^*(t_1) - d_RR^*(t_1)\right]\Delta t + o(\Delta t), \tag{3.48}$$

$$S_{\Delta t}(t_1) = S_0^* + \left[r_S\left(1 - \frac{S_0^* + \alpha R_0^*}{K}\right)S_0^* - d_SS_0^*\right]\Delta t + o(\Delta t), \tag{3.49}$$

$$R_{\Delta t}(t_1) = R_0^* + \left[r_R\left(1 - \frac{\beta S_0^* + R_0^*}{K}\right)R_0^* - d_RR_0^*\right]\Delta t + o(\Delta t), \tag{3.50}$$

$$S_{\Delta t}(t_2) = S_{\Delta t}(t_1) + \left[r_S\left(1 - \frac{S_{\Delta t}(t_1) + \alpha R_{\Delta t}(t_1)}{K}\right)(-\bar{D})S_{\Delta t}(t_1) - d_SS_{\Delta t}(t_1)\right]\Delta t + o(\Delta t), \tag{3.51}$$

$$R_{\Delta t}(t_2) = R_{\Delta t}(t_1) + \left[r_R\left(1 - \frac{\beta S_{\Delta t}(t_1) + R_{\Delta t}(t_1)}{K}\right)R_{\Delta t}(t_1) - d_RR_{\Delta t}(t_1)\right]\Delta t + o(\Delta t). \tag{3.52}$$

And therefore, we have that

$$N^*(T^*) - N_{\Delta t}(T^*) = S^*(t_2) + R^*(t_2) - (S_{\Delta t}(t_2) + R_{\Delta t}(t_2)$$
$$= (1+\bar{D})r_S S_0^* \left(1 - \frac{S_0^* + \alpha R_0^*}{K}\right)\left[d_S + \bar{D}r_S\left(1 - \frac{S_0^* + \alpha R_0^*}{K}\right) + \frac{-\bar{D}r_S S_0^* + r_R \beta R_0^*}{K}\right](\Delta t)^2 + o\left((\Delta t)^2\right). \tag{3.53}$$

Hence, for the case 1, $\alpha = \beta = 1$, it has already been obtained that $1 - \dfrac{S^*(t) + R^*(t)}{K} > 0$ and $\bar{D}r_S S_0^* < r_R R_0^*$ for $\Delta t < \dfrac{T^* - T_0}{2}$ according to Lemma 3.5. And since the $o(\Delta t)$ only depends on the properties of the (assumed) optimal solution $N^*(t)$, there exists a $\delta' < \dfrac{T^* - T_0}{2}$ such that for $\Delta t \in (0, \delta')$, and therefore, $N^*(T^*) - N_{\Delta t}(T^*) > 0$, implying that $N(t)$ reaches $(1+\mu)n_0 K$ at some $t > T^*$, contradicting the assumption that T^* is the optimal objective value.

For the case 2, $1 \le \beta \le \alpha$ and $n_0 < \dfrac{1}{(1+\mu)(1+\beta)}$, it follows that $N^*(T^*) - N_{\Delta t}(T^*) > 0$ by Lemma 3.6, which also contradicts with the assumption that $N^*(t)$ is the optimal state solution.

So the proof has been completed. □

Finally, the proof of Theorem 3.1 is provided.

Proof of Theorem 3.1. We prove by contradiction. For simplicity, let $N(t) = R(t) + S(t)$. Assume that the conclusion does not hold. Since $N(t)$ is a continuous function, the negation of the theorem implies that $N(t) = R(t) + S(t) \le (1+\mu)N(0)$ for all $t \ge 0$.

From the initial condition $N(0) < \dfrac{1}{1+\mu}\left(1 - \dfrac{d_R}{r_R}\right)K$, we have $(1+\mu)N(0) < \left(1 - \dfrac{d_R}{r_R}\right)K$. Therefore, for all $t \ge 0$, the following equation (3.54) holds.

$$N(t) = R(t) + S(t) \le (1+\mu)N(0) < \left(1 - \frac{d_R}{r_R}\right)K. \tag{3.54}$$

Now, consider the differential equation for $R(t)$ as follows,

$$\frac{\mathrm{d}R}{\mathrm{d}t} = r_R\left(1 - \frac{R+S}{K}\right)R - d_R R.$$

Using the assumption that $R(t) + S(t) \le \left(1 - \dfrac{d_R}{r_R}\right)K$, we obtain the following inequality (3.55),

$$\frac{\mathrm{d}R}{\mathrm{d}t} \ge r_R\left(1 - \frac{\left(1 - \dfrac{d_R}{r_R}\right)K}{K}\right)R - d_R R = r_R\left(\frac{d_R}{r_R}\right)R - d_R R = 0. \tag{3.55}$$

Thus, $\dfrac{\mathrm{d}R}{\mathrm{d}t} \ge 0$, so $R(t)$ is non-decreasing. Since $R(0) > 0$, it follows that $R(t) > 0$ for all $t \ge 0$.

Moreover, according to the condition $N(0) = R(0) + S(0) < \frac{1}{1+\mu}\left(1 - \frac{d_R}{r_R}\right)K$, it is reasonable to define the following positive constant,

$$\delta_R = 1 - \frac{d_R}{r_R} - \frac{(1+\mu)N(0)}{K} > 0.$$

Since $R(t) + S(t) \leq (1+\mu)N(0)$ for all $t \geq 0$, the following estimation is obtained as (3.56),

$$\frac{\mathrm{d}R}{\mathrm{d}t} = r_R\left(1 - \frac{R+S}{K}\right)R - d_R R \geq r_R\left(1 - \frac{(1+\mu)N(0)}{K}\right)R - d_R R = r_R\delta_R R, \tag{3.56}$$

which implies that $R(t) \geq R(0)\mathrm{e}^{(r_R\delta_R)t}$ for all $t \geq 0$.

Since $R(0) > 0$ and $r_R\delta_R > 0$, the right-hand side grows exponentially as $t > 0$. However, this contradicts the assumption that $R(t) + S(t) \leq (1+\mu)N(0)$ for all $t \geq 0$.

Therefore, our assumption must be false, and there exists some $T > 0$ such that $N(T) > (1+\mu)N(0)$. This completes the proof. □

4. Discussion

Adaptive therapy crucially leverages competitive dynamics to maintain therapeutic-sensitive cell reservoirs that suppress resistant clones, strategically delaying drug resistance evolution while minimizing tumour progression [21]. By preserving sensitive cells through threshold-modulated treatment holidays, adaptive therapy sustains ecological suppression of resistant populations—an advantage over traditional maximum tolerated dose regimens, which inadvertently accelerate resistance [29]. The clinical success of adaptive therapy hinges on its paradigm-shifting principle: harnessing intra-tumour competition to transform therapy-sensitive cells into permanent controllers of resistant cell expansion [33, 70]. However, the rule-of-thumb thresholds used in clinical practice may require further research and optimisation as they might not fully account for the complex, dynamic interactions between sensitive and resistant cell populations, and may vary across different tumour types and patient profiles [35, 36, 38, 40, 41, 71].

This study employs a Lotka–Volterra model to investigate how treatment-holiday thresholds influence adaptive therapy outcomes in tumours composed of drug-sensitive and resistant cells. By simulating tumour dynamics under varying thresholds, initial tumour burdens, and competition coefficients, the analysis identifies three distinct therapeutic scenarios: **uniform-improve** (where AT consistently outperforms MTD regardless of threshold selection), **conditional-improve** (AT efficacy depends on threshold calibration), and **uniform-decline** (MTD superiority). When considering clinical uncertainties in measurement data, generally, the greater the initial tumour burden, the more likely adaptive therapy will outperform other treatment strategies. However, in cases where the tumour burden is excessively high, the advantages of adaptive therapy become irrelevant, and alternative approaches, beyond pharmacological treatment, may be required.

The competitive dynamics between sensitive and resistant cells is also a key factor in tumour evolution under therapeutic stress. In strong competition environments, tumours tend to evolve toward a state dominated by either sensitive or resistant cells, depending on the initial composition. Continuous MTD therapy drives the tumour toward a stable state where the ratio of sensitive to resistant cells remains constant. Thus, the critical factor in treatment outcomes is not the treatment-holiday threshold but rather the impact of the initial tumour state on the final result. In weak competition environments, sensitive and resistant cells can coexist, and adaptive therapy may lead to resistant cell dominance through Darwinian selection. Treatment effectiveness is influenced by the competition coefficients, α and β, with lower α and higher β favoring adaptive therapy. Adaptive therapy prolongs TTP most effectively when sensitive cells maintain a competitive advantage and when initial tumour burden is high, enabling ecological suppression of resistant cells.

This study advances our understanding of adaptive therapy by systematically quantifying the role of treatment-holiday thresholds in modulating tumour evolution under treatment. By integrating ecological competition principles into therapeutic design, the current work provides a mechanistic basis for optimizing intermittent dosing strategies. The findings highlight that adaptive therapy is not universally superior to MTD; its success depends critically on tumour initial state and the treatment-holiday threshold selection. These insights bridge theoretical ecology and clinical oncology, emphasizing the need for dynamic, patient-specific treatment protocols rather than static dosing regimens.

This work establishes a quantitative relationship between treatment-holiday thresholds and progression-free survival. By categorizing outcomes into three distinct scenarios, the model offers clinicians a potential framework to stratify patients based on measurable parameters such as initial tumour burden and resistant cell fraction. Furthermore, the demonstration that strong competition can stabilize tumour burden indefinitely under specific thresholds has profound implications for managing advanced cancers. These results extend prior work [21, 35, 41, 46] by incorporating threshold-driven mechanism in adaptive therapy.

Despite these advances, the study has several limitations. First, the binary classification of tumour cells overlooks the phenotypic plasticity and continuous heterogeneity that are critical drivers of therapeutic resistance [13, 14, 72]. Second, this study does not explore in depth the scenarios where $\alpha < 0$ or $\beta < 0$, which indicate mutualistic or commensalistic interactions between cell populations. Determining how to refine treatment strategies under these symbiotic states remains an important theoretical question requiring further investigation. Third, model parameters such as the competition coefficients (α, β) are based on population-level assumptions rather than molecular data, necessitating further investigation into the microscopic foundations of these assumptions [73, 74]. Forth, the Lotka–Volterra model does not account for the spatial structure of tumours [75] or the microenvironmental constraints that alter tumour dynamics [76, 77]. Future studies should integrate single-cell and spatial omics data to mechanistically parameterize competition coefficients and explore hybrid models that combine continuum and spatial interactions. Additionally, clinical validation through adaptive therapy trials, incorporating real-time biomarker monitoring, will be crucial for translating these insights into practice.

Funding

This work was funded by The National Natural Science Foundation of China (NSFC) *via* grant 11801020.

Data availability statement

- This study did not use any real-world data; all data were generated through computational simulations.
- All original code has been deposited on GitHub (`https://github.com/zhuge-c/AT-0`).
- Any additional information required to re the data reported in this paper is available from the last contact upon request.

References

[1] F. Bray, M. Laversanne, H. Sung, J. Ferlay, R.L. Siegel, I. Soerjomataram and A. Jemal, Global cancer statistics 2022: GLOBOCAN estimates of incidence and mortality worldwide for 36 cancers in 185 countries. *CA Cancer J. Clin.* **74** (2024) 229–263.

[2] A. Marusyk, V. Almendro and K. Polyak, Intra-tumour heterogeneity: a looking glass for cancer? *Nat. Rev. Cancer* **12** (2012) 323–334.

[3] C.E. Meacham and S.J. Morrison, Tumour heterogeneity and cancer cell plasticity. *Nature* **501** (2013) 328–337.

[4] H. Sung, J. Ferlay, R.L. Siegel, M. Laversanne, I. Soerjomataram, A. Jemal and F. Bray, Global Cancer Statistics 2020: GLOBOCAN Estimates of Incidence and Mortality Worldwide for 36 Cancers in 185 Countries. *CA Cancer J. Clin.* **71** (2021) 209–249.

[5] C. Holohan, S. Van Schaeybroeck, D.B. Longley and P.G. Johnston, Cancer drug resistance: an evolving paradigm. *Nat. Rev. Cancer* **13** (2013) 714–726.

[6] S.V. Sharma, D.Y. Lee, B. Li, M.P. Quinlan, F. Takahashi, S. Maheswaran, U. McDermott, N. Azizian, L. Zou, M.A. Fischbach, K.K. Wong, K. Brandstetter, B. Wittner, S. Ramaswamy, M. Classon and J. Settleman, A chromatin-mediated reversible drug-tolerant state in cancer cell subpopulations. *Cell* **141** (2010) 69–80.

[7] Z.-D. Shi, K. Pang, Z.-X. Wu, Y. Dong, L. Hao, J.-X. Qin, W. Wang, Z.-S. Chen and C.-H. Han, Tumor cell plasticity in targeted therapy-induced resistance: mechanisms and new strategies. *Signal Transduct. Target. Ther.* **8** (2023) 113.

[8] Y. Tian, X. Wang, C. Wu, J. Qiao, H. Jin and H. Li, A protracted war against cancer drug resistance. *Cancer Cell Int.* **24** (2024) 326.

[9] X. Wang, H. Zhang and X. Chen, Drug resistance and combating drug resistance in cancer. *Cancer Drug Resist.* **2** (2019) 141–160.

[10] M. Greaves and C.C. Maley, Clonal evolution in cancer. *Nature* **481** (2012) 306–313.

[11] N. McGranahan and C. Swanton, Clonal heterogeneity and tumor evolution: past, present, and the future. *Cell* **168** (2017) 613–628.

[12] S. Turajlic, A. Sottoriva, T. Graham and C. Swanton, Resolving genetic heterogeneity in cancer. *Nat. Rev. Genet.* **20** (2019) 404–416.

[13] P.B. Gupta, C.M. Fillmore, G. Jiang, S.D. Shapira, K. Tao, C. Kuperwasser and E.S. Lander, Stochastic state transitions give rise to phenotypic equilibrium in populations of cancer cells. *Cell* **146** (2011) 633–644.

[14] A. Marusyk, M. Janiszewska and K. Polyak, Intratumor heterogeneity: the rosetta stone of therapy resistance. *Cancer Cell* **37** (2020) 471–484.

[15] G. Aguadé-Gorgorió, A.R.A. Anderson and R. Solé, Modeling tumors as complex ecosystems. *iScience* **27** (2024) 110699.

[16] D. Bilder, K. Ong, T.C. Hsi, K. Adiga and J. Kim, Tumour–host interactions through the lens of Drosophila. *Nat. Rev. Cancer* **21** (2021) 687–700.

[17] R. Brady and H. Enderling, Mathematical models of cancer: when to predict novel therapies, and when not to. *Bull. Math. Biol.* **81** (2019) 3722–3731.

[18] J.S. Brown, S.R. Amend, R.H. Austin, R.A. Gatenby, E.U. Hammarlund and K.J. Pienta, Updating the definition of cancer. *Mol. Cancer Res.* **21** (2023) 1142–1147.

[19] A. Bukkuri, K.J. Pienta, I. Hockett, R.H. Austin, E.U. Hammarlund, S.R. Amend and J.S. Brown, Modeling cancer's ecological and evolutionary dynamics. *Med. Oncol.* **40** (2023) 109.

[20] R.A. Gatenby, A change of strategy in the war on cancer. *Nature* **459** (2009) 508–509.

[21] R.A. Gatenby, A.S. Silva, R.J. Gillies and B. Roy Frieden, Adaptive therapy. *Cancer Res.* **69** (2009) 4894–4903.

[22] M.E. Hochberg, An ecosystem framework for understanding and treating disease. *Evol. Med. Public Health* (2018) 270–286.

[23] N. Zahir, R. Sun, D. Gallahan, R.A. Gatenby and C. Curtis, Characterizing the ecological and evolutionary dynamics of cancer. *Nat. Genet.* **52** (2020) 759–767.

[24] C. Stephan-Otto Attolini and F. Michor, Evolutionary Theory of Cancer. *Ann. N. Y. Acad. Sci.* **1168** (2009) 23–51.

[25] N. Vasan, J. Baselga and D.M. Hyman, A view on drug resistance in cancer. *Nature* **575** (2019) 299–309.

[26] M. Pressley, M. Salvioli, D.B. Lewis, C.L. Richards, J.S. Brown and K. Staňková, Evolutionary dynamics of treatment-induced resistance in canceR informs understanding of rapid evolution in natural systems. *Front. Ecol. Evol.* **9** (2021) 1–22.

[27] J. Zhang, J. Cunningham, J. Brown and R. Gatenby, Evolution-based mathematical models significantly prolong response to abiraterone in metastatic castrate-resistant prostate cancer and identify strategies to further improve outcomes. *eLife* **11** (2022) 1–105.

[28] C. Athena Aktipis, A.M. Boddy, G. Jansen, U. Hibner, M.E. Hochberg, C.C. Maley, G.S. Wilkinson, C. Athena Aktipis, A.M. Boddy, G. Jansen, U. Hibner, M.E. Hochberg, C.C. Maley and G.S. Wilkinson, Cancer across the tree of life: cooperation and cheating in multicellularity. *Philos. Trans. Roy. Soc. B: Biol. Sci.* **370** (2015) 20140219.

[29] P.M. Enriquez-Navas, Y. Kam, T. Das, S. Hassan, A. Silva, P. Foroutan, E. Ruiz, G. Martinez, S. Minton, R.J. Gillies and R.A. Gatenby, Exploiting evolutionary principles to prolong tumor control in preclinical models of breast cancer. *Sci. Transl. Med.* **8** (2016).

[30] C.C. Maley, A. Aktipis, T.A. Graham, A. Sottoriva, A.M. Boddy, M. Janiszewska, A.S. Silva, M. Gerlinger, Y. Yuan, K.J. Pienta, K.S. Anderson, R. Gatenby, C. Swanton, D. Posada, C.-I. Wu, J.D. Schiffman, E. Shelley Hwang, K.

Polyak, A.R.A. Anderson, J.S. Brown, M. Greaves and D. Shibata, Classifying the evolutionary and ecological features of neoplasms. *Nat. Rev. Cancer* **17** (2017) 605–619.

[31] J. West, F. Adler, J. Gallaher, M. Strobl, R. Brady-Nicholls, J. Brown, M. Roberson-Tessi, E. Kim, R. Noble, Y. Viossat, D. Basanta and A.R.A. Anderson, A survey of open questions in adaptive therapy: bridging mathematics and clinical translation. *eLife* **12** (2023) 1–25.

[32] J.A. Gallaher, P.M. Enriquez-Navas, K.A. Luddy, R.A. Gatenby and A.R.A. Anderson, Spatial heterogeneity and evolutionary dynamics modulate time to recurrence in continuous and adaptive cancer therapies. *Cancer Res.* **78** (2018) 2127–2139.

[33] J. West, L. You, J. Zhang, R.A. Gatenby, J.S. Brown, P.K. Newton and A.R.A. Anderson, Towards multidrug adaptive therapy. *Cancer Res.* **80** (2020) 1578–1589.

[34] P.M. Enriquez-Navas, J.W. Wojtkowiak and R.A. Gatenby, Application of evolutionary principles to cancer therapy. *Cancer Res.* **75** (2015) 4675–4680.

[35] C. McGehee and Y. Mori, A mathematical framework for comparison of intermittent versus continuous adaptive chemotherapy dosing in cancer. *npj Syst. Biol. Appl.* **10** (2024) 140.

[36] M.A.R. Strobl, J. Gallaher, M. Robertson-Tessi, J. West and A.R.A. Anderson, Treatment of evolving cancers will require dynamic decision support. *Ann. Oncol.* **34** (2023) 867–884.

[37] J. Zhang, J.J. Cunningham, J.S. Brown and R.A. Gatenby, Integrating evolutionary dynamics into treatment of metastatic castrate-resistant prostate cancer. *Nat. Commun.* **8** (2017) 1–9.

[38] B. Liu, H. Zhou, L. Tan, K. To Hugo Siu and X.-Y. Guan, Exploring treatment options in cancer: tumor treatment strategies. *Signal Transduct. Target. Ther.* **9** (2024) 175.

[39] M.A.R. Strobl, A.L. Martin, J. West, J. Gallaher, M. Robertson-Tessi, R. Gatenby, R. Wenham, P.K. Maini, M. Damaghi and A.R.A. Anderson, To modulate or to skip: Fe-escalating PARP inhibitor maintenance therapy in ovarian cancer using adaptive therapy. *Cell Syst.* **15** (2024) 510–525.

[40] R.Z. Tan, Tumour Growth Mechanisms Determine Effectiveness of Adaptive Therapy in Glandular Tumours. *Interdiscipl. Sci. Computat. Life Sci.* **16** (2024) 73–90.

[41] M.Y. Wang, J.G. Scott and A. Vladimirsky, Threshold-awareness in adaptive cancer therapy. *PLoS Computat. Biol.* **20** (2024) e1012165.

[42] R.A. Beckman, I. Kareva and F.R. Adler, How should cancer models be constructed? *Cancer Control* **27** (2020) 1–12.

[43] K. Gallagher, M.A.R. Strobl, D.S. Park, F.C. Spoendlin, R.A. Gatenby, P.K. Maini and A.R.A. Anderson, Mathematical model-driven deep learning enables personalized adaptive therapy. *Cancer Res.* **84** (2024) 1929–1941.

[44] R.A. Gatenby and T.L. Vincent, Application of quantitative models from population biology and evolutionary game theory to tumor therapeutic strategies. *Mol. Cancer Ther.* **2** (2003) 919–927.

[45] D. Mathur, E. Barnett, H.I. Scher and J.B. Xavier, Optimizing the future: how mathematical models inform treatment schedules for cancer. *Trends Cancer* **8** (2022) 506–516.

[46] M.A.R. Strobl, J. West, Y. Viossat, M. Damaghi, M. Robertson-Tessi, J.S. Brown, R.A. Gatenby, P.K. Maini and A.R.A. Anderson, Turnover modulates the need for a cost of resistance in adaptive therapy. *Cancer Res.* **81** (2021) 1135–1147.

[47] Y. Deng, L. Xia, J. Zhang, S. Deng, M. Wang, S. Wei, K. Li, H. Lai, Y. Yang, Y. Bai, Y. Liu, L. Luo, Z. Yang, Y. Chen, R. Kang, F. Gan, Q. Pu, J. Mei, L. Ma, F. Lin, C. Guo, H. Liao, Y. Zhu, Z. Liu, C. Liu, Y. Hu, Y. Yuan, Z. Zha, G. Yuan, G. Zhang, L. Chen, Q. Cheng, S. Shen and L. Liu, Multicellular ecotypes shape progression of lung adenocarcinoma from ground-glass opacity toward advanced stages. *Cell Rep. Med.* (2024) 101489.

[48] L. Ermini, S. Taurone, A. Greco and M. Artico, Cancer progression: a single cell perspective. *Eur. Rev. Med. Pharmacol. Sci.* **27** (2023) 5721–5747.

[49] E. Pennisi, Is cancer a breakdown of multicellularity? *Science* **360** (2018) 1391–1391.

[50] G. Aguadé-Gorgorió and S. Kéfi, Alternative cliques of coexisting species in complex ecosystems. *J. Phys. Complex.* **5** (2024).

[51] A. Chapman, L.F. del Ama, J. Ferguson, J. Kamarashev, C. Wellbrock and A. Hurlstone, Heterogeneous tumor subpopulations cooperate to drive invasion. *Cell Rep.* **8** (2014) 688–695.

[52] R. Emond, J.I. Griffiths, V.K. Grolmusz, A. Nath, J. Chen, E.F. Medina, R.S. Sousa, T. Synold, F.R. Adler and A.H. Bild, Cell facilitation promotes growth and survival under drug pressure in breast cancer. *Nat. Commun.* **14** (2023) 3851.

[53] M.A. Masud, J.-Y. Kim, C.-H. Pan and E. Kim, The impact of the spatial heterogeneity of resistant cells and fibroblasts on treatment response. *PLoS Computat. Biol.* **18** (2022) e1009919.

[54] M. Robertson-Tessi, B. Desai, T. Miti, P. Kumar, S. Yarlagadda, R. Shah, R.V. Velde, D. Miroshnychenko, D. Basanta, A. Anderson and A. Marusyk, Abstract B008: Therapy-protective peristromal niches mediate positive ecological interaction between therapy-sensitive and therapy-resistant cells, altering the evolutionary dynamics of acquired targeted therapy resistance in lung cancers. *Cancer Res.* **84** (2024) B008–B008.

[55] S. Seyedi, R. Teo, L. Foster, D. Saha, L. Mina, D. Northfelt, K.S. Anderson, D. Shibata, R. Gatenby, L.H. Cisneros, B. Troan, A.R.A. Anderson and C.C. Maley, Testing adaptive therapy protocols using gemcitabine and capecitabine in a preclinical model of endocrine-resistant breast cancer. *Cancers* **16** (2024) 257.

[56] I. Smalley, E. Kim, J. Li, P. Spence, C.J. Wyatt, Z. Eroglu, V.K. Sondak, J.L. Messina, N.A. Babacan, S.S. Maria-Engler, L. De Armas, S.L. Williams, R.A. Gatenby, Y. Ann Chen, A.R.A. Anderson and K.S.M. Smalley, Leveraging transcriptional dynamics to improve BRAF inhibitor responses in melanoma. *EBioMedicine* **48** (2019) 178–190.

[57] C. Grassberger, D. McClatchy, C. Geng, S.C. Kamran, F. Fintelmann, Y.E. Maruvka, Z. Piotrowska, H. Willers, L.V. Sequist, A.N. Hata and H. Paganetti, Patient-specific tumor growth trajectories determine persistent and resistant cancer cell populations during treatment with targeted therapies. *Cancer Res.* **79** (2019) 3776–3788.

[58] E.D. Sunassee, D. Tan, N. Ji, R. Brady, E.G. Moros, J.J. Caudell, S. Yartsev and H. Enderling, Proliferation saturation index in an adaptive Bayesian approach to predict patient-specific radiotherapy responses. *Int. J. Radiat. Biol.* **95** (2019) 1421–1426.

[59] J.B. West, M.N. Dinh, J.S. Brown, J. Zhang, A.R. Anderson and R.A. Gatenby, Multidrug cancer therapy in metastatic castrate-resistant prostate cancer: an evolution-based strategy. *Clin. Cancer Res.* **25** (2019) 4413–4421.

[60] R. Simon and L. Norton, The Norton-–Simon hypothesis: designing more effective and less toxic chemotherapeutic regimens. *Nat. Clin. Pract. Oncol.* **3** (2006) 406–407.

[61] T.A. Traina and L. Norton, Norton–Simon hypothesis, in *Encyclopedia of Cancer*. Springer Berlin Heidelberg, Berlin, Heidelberg (2011) 2557–2559.

[62] Y. Viossat and R. Noble, A theoretical analysis of tumour containment. *Nat. Ecol. Evol.* **5** (6) 826–835.

[63] E. Hansen and A.F. Read, Modifying adaptive therapy to enhance competitive suppression. *Cancers* **12** (2020) 3556.

[64] R. Gatenby and J. Brown, The evolution and ecology of resistance in cancer therapy. *Cold Spring Harbor Perspect. Med.* **8** (2018).

[65] J. Park and P.K. Newton, Stochastic competitive release and adaptive chemotherapy. *Phys. Rev. E* **108** (2023) 034407.

[66] T.M. Parker, K. Gupta, A.M. Palma, M. Yekelchyk, P.B. Fisher, S.R. Grossman, K.J. Won, E. Madan, E. Moreno and R. Gogna, Cell competition in intratumoral and tumor microenvironment interactions. *EMBO J.* **40** (2021) 1–15.

[67] T. Wang and X. Zou, Dynamic analysis of a drug resistance evolution model with nonlinear immune response. *Math. Biosci.* **374** (2024) 109239.

[68] B. Tang, Y. Xiao and J. Wu, Dynamic behaviors of a periodic system with threshold policy-guided periodic and intermittent therapy of tumor. *SIAM J. Appl. Math.* **85** (2025) 366–392.

[69] D. Wang and J. Lei, Optimal adaptive therapeutic schedules for metastatic castrate-resistant prostate cancer based on bilevel optimization problem. *J. Math. Biol.* **90** (2025) 60.

[70] Y. Zhang, T. Vu, D.C. Palmer, R.J. Kishton, L. Gong, J. Huang, T. Nguyen, Z. Chen, C. Smith, F. Livák, R. Paul, C.-p. Day, C. Wu, G. Merlino, K. Aldape, X.-y. Guan and P. Jiang, A T cell resilience model associated with response to immunotherapy in multiple tumor types. *Nat. Med.* **28** (2022) 1421–1431.

[71] M. Strobl, A.L. Martin, J. West, J. Gallaher, M. Robertson-Tessi, R. Gatenby, R. Wenham, P. Maini, M. Damaghi and A. Anderson, Adaptive therapy for ovarian cancer: An integrated approach to PARP inhibitor scheduling. bioRxiv (2023).

[72] T. Brabletz, R. Kalluri, M.A. Nieto and R.A. Weinberg, EMT in cancer. *Nat. Rev. Cancer* **18** (2018) 128–134.

[73] A. Uthamacumaran and H. Zenil, A review of mathematical and computational methods in cancer dynamics. *Front. Oncol.* **12** (2022) 1–26.

[74] F.-S. Wang and C. Zhang, What to do next to control the 2019-nCoV epidemic? *Lancet* **395** (2022) 391–393.

[75] R. Noble, D. Burri, C. Le Sueur, J. Lemant, Y. Viossat, J. N. Kather and N. Beerenwinkel. Spatial structure governs the mode of tumour evolution. *Nat. Ecol. Evol.* **6** (2021) 207–217.

[76] T. Lorenzi, R.H. Chisholm and J. Clairambault, Tracking the evolution of cancer cell populations through the mathematical lens of phenotype-structured equations. *Biol. Direct* **11** (2016) 43.

[77] J. West, Y. Ma and P.K. Newton, Capitalizing on competition: an evolutionary model of competitive release in metastatic castration resistant prostate cancer treatment. *J. Theoret. Biol.* **455** (2018) 249–260.

Appendix A. Details of the dependence of TTP on various parameters in neutral competition condition

By varying the initial proportion of resistant cells and the initial total tumour burden under different treatment-holiday thresholds (Fig. S2A1-A3), we observed that when the initial total tumour burden is small and the initial proportion of resistant cells is high, the TTP is short. In this case, although the tumour size is small, it contains a large proportion of resistant cells, making it difficult for sensitive cells to suppress resistant cells, and thus cancer becomes harder to treat. As the initial total tumour burden increases and the initial proportion of resistant cells decreases, the TTP gradually increases. At this stage, although the number of resistant cells is low, the tumour is larger, requiring multiple treatment cycles in adaptive therapy to suppress resistant cells. Overall, larger adaptive thresholds, higher initial total tumour burdens, and lower initial proportions of resistant cells result in better treatment outcomes.

By varying the treatment-holiday threshold for dose-skipping and the initial proportion of resistant cells under different initial total cell proportions (Fig. S2B1-B3), we found that lower treatment-holiday thresholds and higher initial proportions of resistant cells result in shorter TTPs. This is because tumours containing a high proportion of resistant cells make it difficult for adaptive therapy to reduce the total tumour burden below the threshold. As the adaptive threshold increases and the initial proportion of resistant cells decreases, the TTP gradually increases. When the adaptive threshold is high and the initial proportion of resistant cells is low, the TTP is maximized. At this stage, the tumour contains a significant number of sensitive cells, and a high threshold adaptive therapy can increase the number of treatment cycles, fully utilizing sensitive cells to suppress resistant cell growth. Overall, higher initial total tumour burdens are associated with longer TTPs.

By varying the treatment-holiday threshold for dose modulation and the initial total tumour burden under different initial proportions of resistant cells (Fig. S2C1-C3), we observed that lower treatment-holiday thresholds and lower initial total tumour burdens result in shorter TTPs. This occurs because, despite the smaller tumour size, the low adaptive threshold leads to prolonged treatment cycles, causing significant damage to sensitive cells and reducing their ability to suppress resistant cells, resulting in shorter TTPs. As the adaptive threshold increases and the initial total tumour burden rises, the TTP gradually increases. When the adaptive threshold and the initial total tumour burden are both high, the TTP is maximized. At this stage, although the tumour size is large, the shorter treatment cycles allow sensitive cells sufficient time to recover and suppress resistant cell growth, resulting in longer TTPs. Overall, lower initial proportions of resistant cells are associated with longer TTPs.

Under the same conditions, simulations that varied the growth rates of sensitive and resistant cells revealed that when the ratio of the growth rate of sensitive cells to resistant cells (r_S/r_R) is greater than 1, indicating that the growth rate of sensitive cells exceeds that of resistant cells, the sensitive cells exhibit stronger competitiveness, resulting in longer TTPs. Conversely, when the ratio is less than 1, indicating that the growth rate of resistant cells exceeds that of sensitive cells, the TTP is shorter, and the higher the growth rate of resistant cells, the shorter the TTP. This relationship is illustrated in Figures S3 through S7.

Appendix B. Details of comparison of adaptive therapy with other strategies in the weak competition condition

To investigate the probability of selecting adaptive therapy under varying parameters, we randomly varied five key model parameters from Table 1, creating a cohort of 1200 virtual patients. Simulations across different initial tumour burdens revealed that as the initial tumour burden increases, the probability of selecting adaptive therapy also increases (Main Text Fig. 6D1-D7). However, when the competition coefficients satisfy $\alpha > 1$ and $\beta > 1$, and the initial tumour burden approaches the carrying capacity, the probability of selecting adaptive therapy decreases (Main Text Fig. 6D8). This is because, under high competition coefficients, tumour competition becomes intense, and both MTD and adaptive therapy can control tumour size indefinitely, leading to a lower probability of selecting adaptive therapy with adaptive therapy (Fig. S11).

In the case of conditional-improve, the differences in treatment outcomes among the four optimal strategies are small (approximately one month; $C_{\mathrm{TH0}} = 0.98$, $(\delta_1, \delta_2, C_{\mathrm{TH2}} - 1, C_{\mathrm{TH1}} - 1) = (0.25, 0.25, 0.05, 0.07)$, $(T_D, T) = (9, 10)$). Since intermittent therapy requires a treatment holiday, the calculation of its optimal cycle revealed a one-day treatment holiday, resulting in treatment outcomes similar to MTD (Fig. S8A). Considering cumulative drug toxicity, AT-S demonstrates the best efficiency among the four strategies (Fig. S8B).

Subsequently, we varied the initial tumour parameters to the treatment outcomes of the four strategies. When the initial proportion of resistant cells remains constant, and the initial tumour burden is small, the differences in TTP extension among the strategies are minimal. As the initial tumour burden increases, AT-S outperforms the other strategies in extending TTP, while AT-M shows the best Relative efficiency (Fig. S8C).

When the initial tumour burden remains constant, and the initial proportion of resistant cells is small, AT-S outperforms the other strategies. However, as the initial proportion of resistant cells increases, MTD, AT-S, and IT outperform AT-M, with AT-S and AT-M demonstrating the best Relative efficiency among the four strategies (Fig. S8D).

For the uniform-improve scenario, the differences in treatment outcomes among the four optimal strategies are minimal (approximately one month; $C_{\mathrm{TH0}} = 0.98$, $(\delta_1, \delta_2, C_{\mathrm{TH2}} - 1, C_{\mathrm{TH1}} - 1) = (0.25, 0.25, 0.05, 0.09)$, $(T_D, T) = (20, 21)$). Similar to the conditional-improve scenario, the optimal intermittent therapy cycle includes a one-day treatment holiday, resulting in treatment outcomes similar to MTD (Fig. S9A). Considering cumulative drug toxicity, AT-S shows the best efficiency among the four strategies (Fig. S9B).

When varying the initial total tumour burden while keeping the initial proportion of resistant cells constant, the differences in TTP extension among the four strategies are minor. MTD and IT outperform AT-S and AT-M in terms of TTP, but AT-S and AT-M have a better relative efficiency than MTD and IT (Fig. S9C). When varying the initial proportion of resistant cells while keeping the initial tumour burden constant, MTD and IT outperform AT-S and AT-M in terms of TTP. However, AT-S and AT-M exhibit a better Relative efficiency compared to MTD and IT (Fig. S9D).

For the uniform-decline scenario, the differences in TTP among the four optimal strategies are larger (approximately two months; $C_{\mathrm{TH0}} = 0.98$, $(\delta_1, \delta_2, C_{\mathrm{TH2}} - 1, C_{\mathrm{TH1}} - 1) = (0.25, 0.25, 0.05, 0.05)$, $(T_D, T) = (15, 18)$). Among the four strategies, AT-S and AT-M demonstrate the best treatment outcomes (Fig. S10A). Regarding cumulative drug toxicity, AT-S achieves the best relative efficiency (Fig. S10B).

When varying the initial total tumour burden while keeping the initial proportion of resistant cells constant, the differences in treatment outcomes are minor for small tumours. For larger tumours, AT-S shows the best treatment outcomes, while AT-M and AT-S have a better Relative efficiency than the other two strategies (Fig. S10C). When varying the initial proportion of resistant cells while keeping the initial tumour burden constant, AT-S demonstrates the best treatment outcomes regardless of the proportion of resistant cells. AT-M shows slightly worse treatment outcomes than the other three strategies but exhibits the best Relative efficiency (Fig. S10D).

Appendix C. Supplementary figures

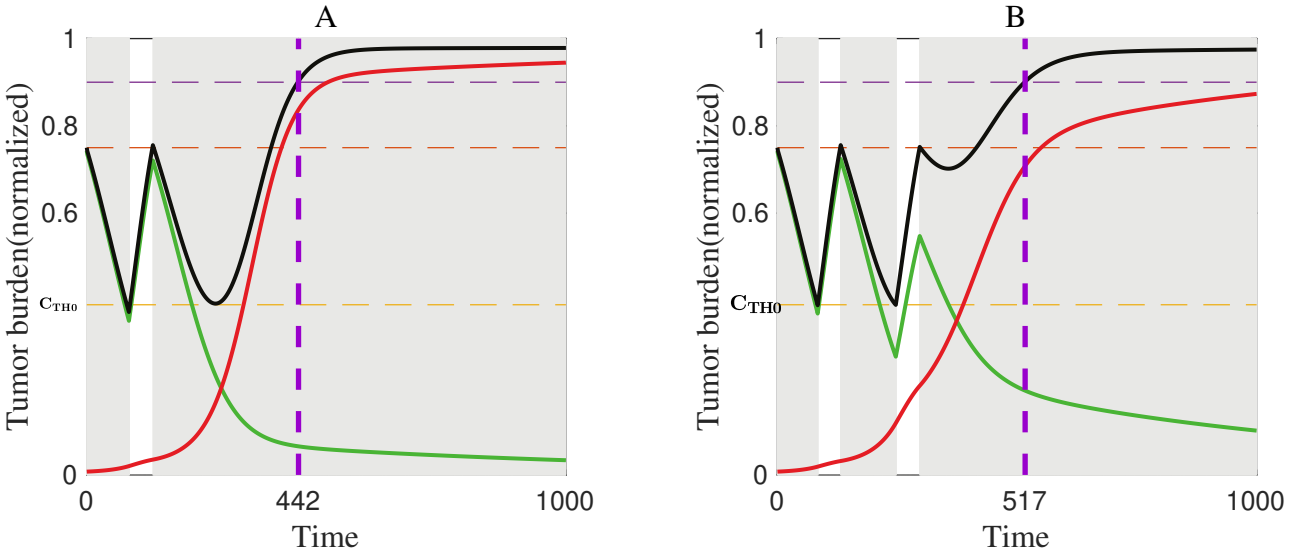

Figure S1. tumour evolution dynamics in neutral competition with different treatment-holiday thresholds, showing the reason of discontinuity in the dependence of TTP on the treatment-holiday thresholds (Fig. 2). Purple dashed line: TTP; Red: Resistant cells; Green: Sensitive cells; Black: Total tumour burden; Shaded area: Treatment implementation. **(A)** $n_0 = 0.75$, $f_R = 0.01$, $C_{\mathrm{TH0}} = 0.51$. **(B)** $n_0 = 0.75$, $f_R = 0.01$, $C_{\mathrm{TH0}} = 0.52$. Other parameters are taken as those in Table 1.

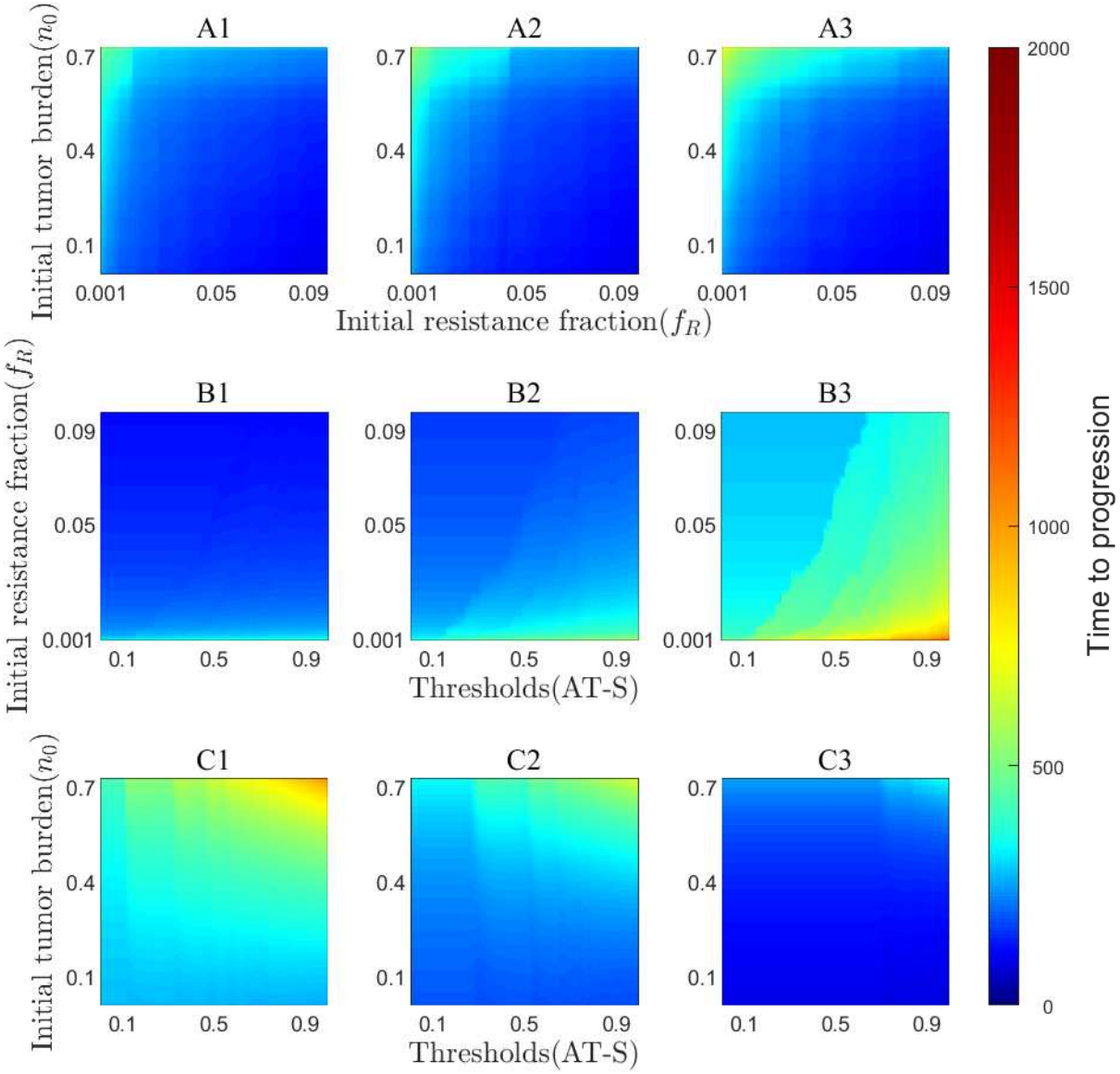

FIGURE S2. The impact of initial tumour state and treatment-holiday thresholds on TTP. **(A1)-(A3)** The effect of varying the initial proportion of resistant cells and the initial total tumour burden on TTP at fixed adaptive thresholds. A1: $C_{\mathrm{TH0}} = 0.3$; A2: $C_{\mathrm{TH0}} = 0.5$; A3: $C_{\mathrm{TH0}} = 0.8$. **(B1)-(B3)** The effect of varying treatment-holiday thresholds and the initial proportion of resistant cells on TTP at fixed initial . B1: $n_0 = 0.25$; B2: $n_0 = 0.5$; B3: $n_0 = 0.75$. **(C1)-(C3)** The effect of varying treatment-holiday thresholds and initial tumour burdens on TTP at fixed proportions of resistant cells. C1: $f_R = 0.001$; C2: $f_R = 0.01$; C3: $f_R = 0.1$.

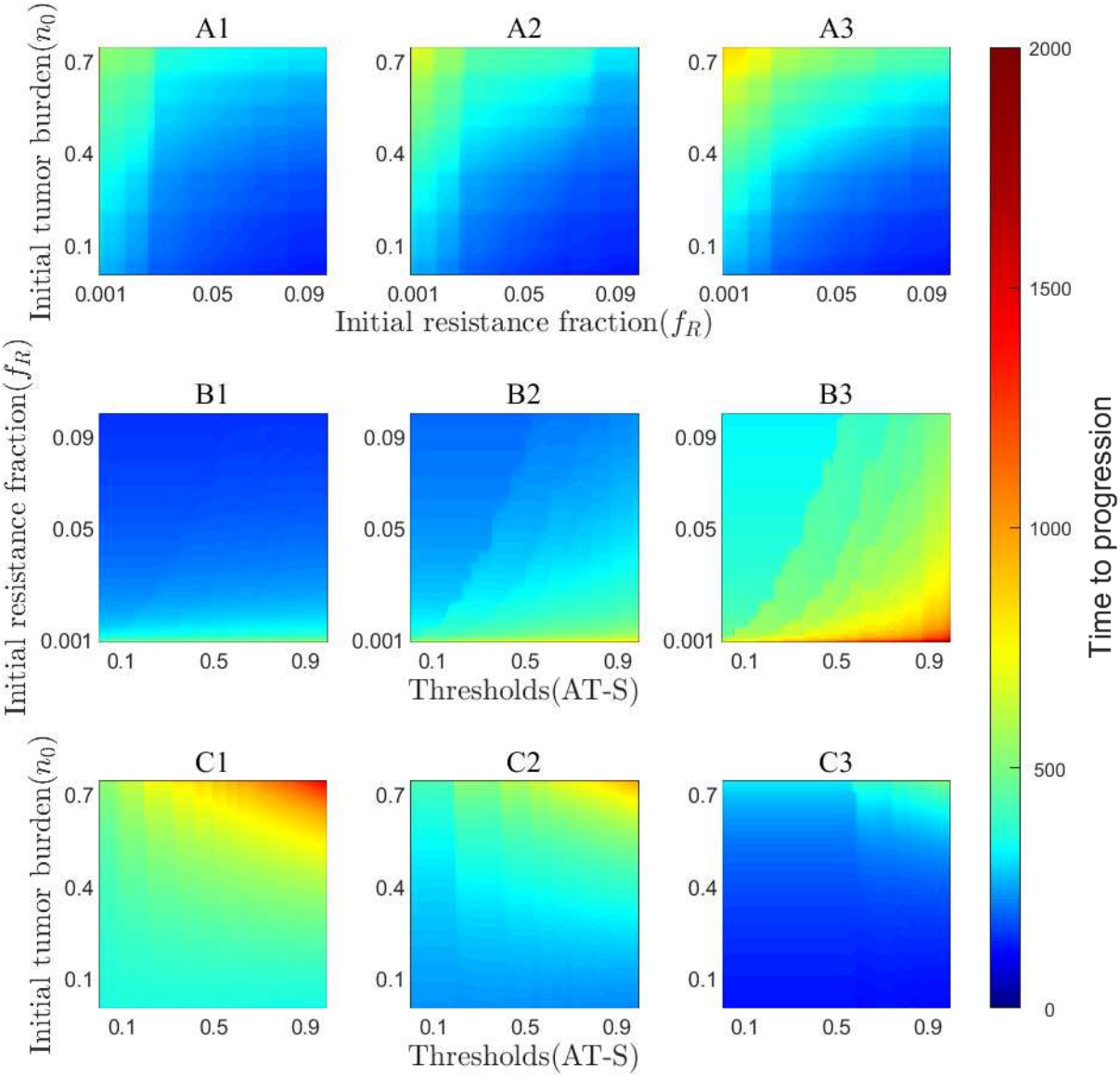

FIGURE S3. The dependence of TTP on the thresholds, initial tumour burden (n_0) and initial fraction of resistant cells (f_R) in neutral competition with $r_S/r_R = 1.8863$, $r_S = 0.0389$. **(A1)-(A3)** Effects of varying initial resistance proportions and tumour burdens on TTP, A1: $C_{\mathrm{TH0}} = 0.3$; A2: $C_{\mathrm{TH0}} = 0.5$; A3: $C_{\mathrm{TH0}} = 0.8$ **(B1)-(B3)** Effects of varying treatment-holiday thresholds and initial resistance proportions on TTP. B1: $n_0 = 0.25$; B2: $n_0 = 0.5$; B3: $n_0 = 0.75$ **(C1)-(C3)** Effects of varying treatment-holiday thresholds and initial tumour burden on TTP, C1: $f_R = 0.001$; C2: $f_R = 0.01$; C3: $f_R = 0.1$.

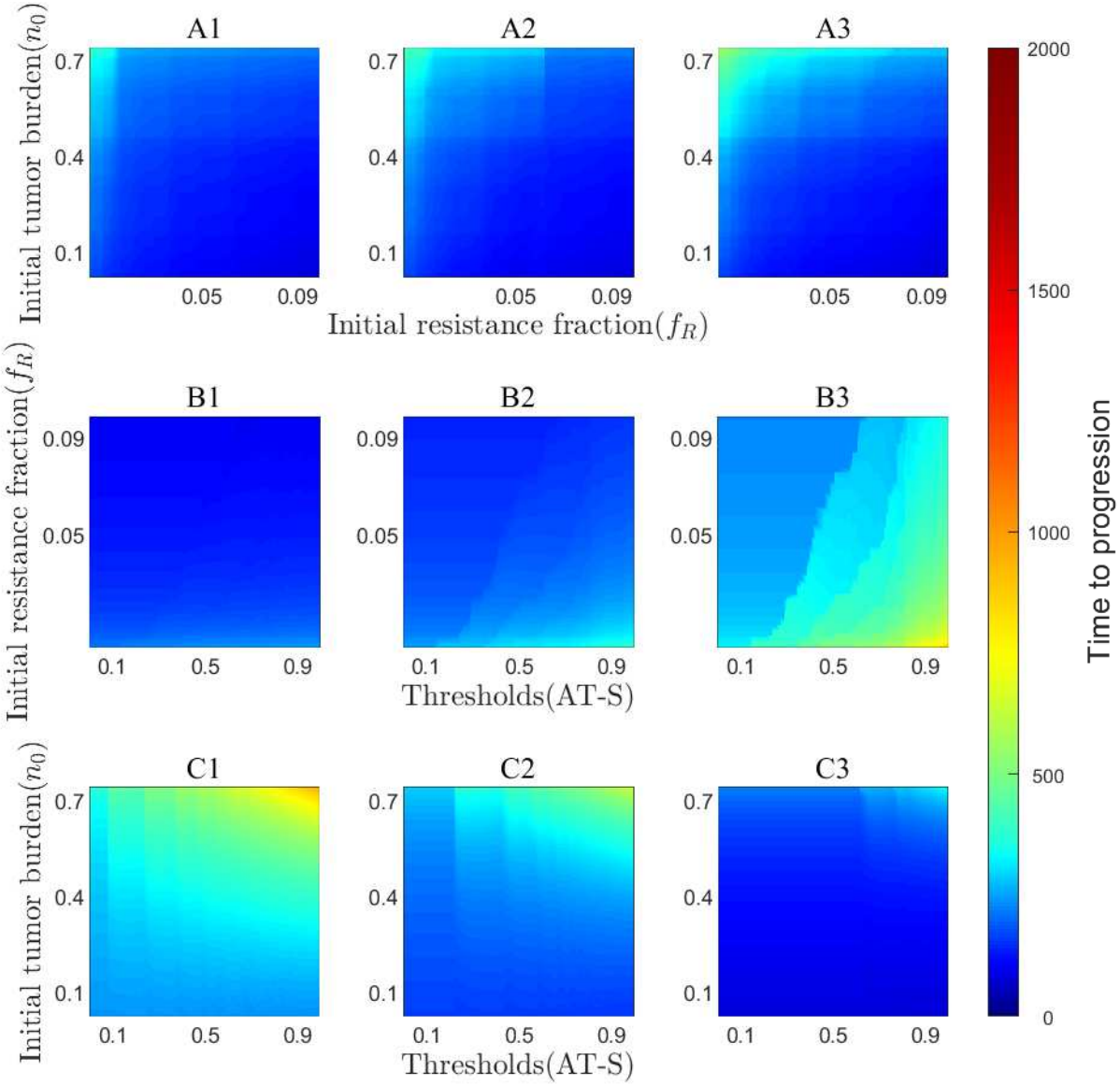

FIGURE S4. The dependence of TTP on the thresholds, initial tumour burden (n_0) and initial fraction of resistant cells (f_R) in neutral competition with $r_S/r_R = 1.6493$, $r_S = 0.0508$. **(A1)-(A3)** Effects of varying initial resistance proportions and tumour burdens on TTP, A1: $C_{\mathrm{TH0}} = 0.3$; A2: $C_{\mathrm{TH0}} = 0.5$; A3: $C_{\mathrm{TH0}} = 0.8$ **(B1)-(B3)** Effects of varying treatment-holiday thresholds and initial resistance proportions on TTP. B1: $n_0 = 0.25$; B2: $n_0 = 0.5$; B3: $n_0 = 0.75$ **(C1)-(C3)** Effects of varying treatment-holiday thresholds and initial tumour burden on TTP, C1: $f_R = 0.001$; C2: $f_R = 0.01$; C3: $f_R = 0.1$.

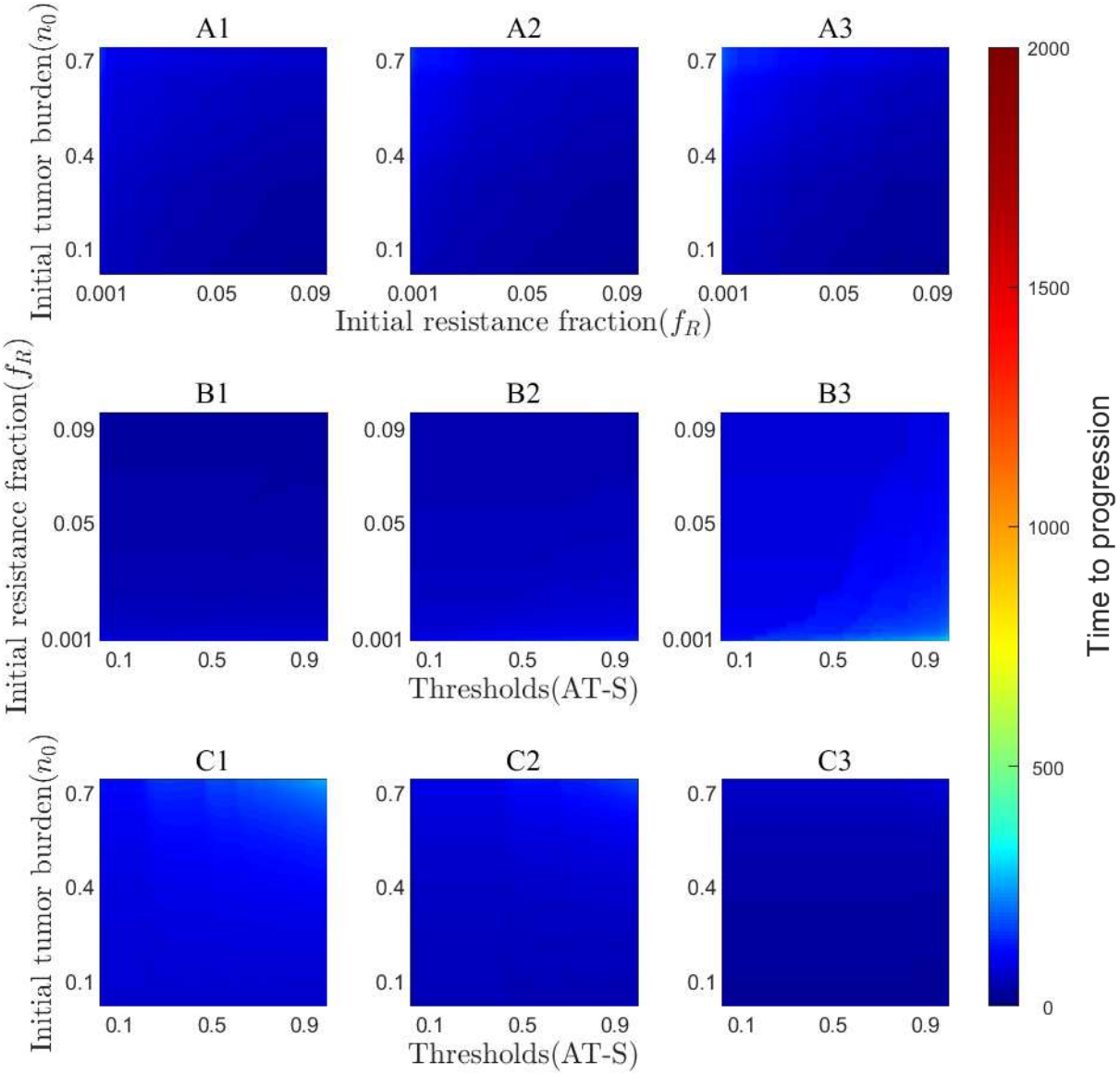

FIGURE S5. The dependence of TTP on the thresholds, initial tumour burden (n_0) and initial fraction of resistant cells (f_R) in neutral competition with $r_S/r_R = 0.8147$, $r_S = 0.0915$. **(A1)-(A3)** Effects of varying initial resistance proportions and tumour burdens on TTP, A1: $C_{\mathrm{TH0}} = 0.3$; A2: $C_{\mathrm{TH0}} = 0.5$; A3: $C_{\mathrm{TH0}} = 0.8$ **(B1)-(B3)** Effects of varying treatment-holiday thresholds and initial resistance proportions on TTP. B1: $n_0 = 0.25$; B2: $n_0 = 0.5$; B3: $n_0 = 0.75$ **(C1)-(C3)** Effects of varying treatment-holiday thresholds and initial tumour burden on TTP, C1: $f_R = 0.001$; C2: $f_R = 0.01$; C3: $f_R = 0.1$.

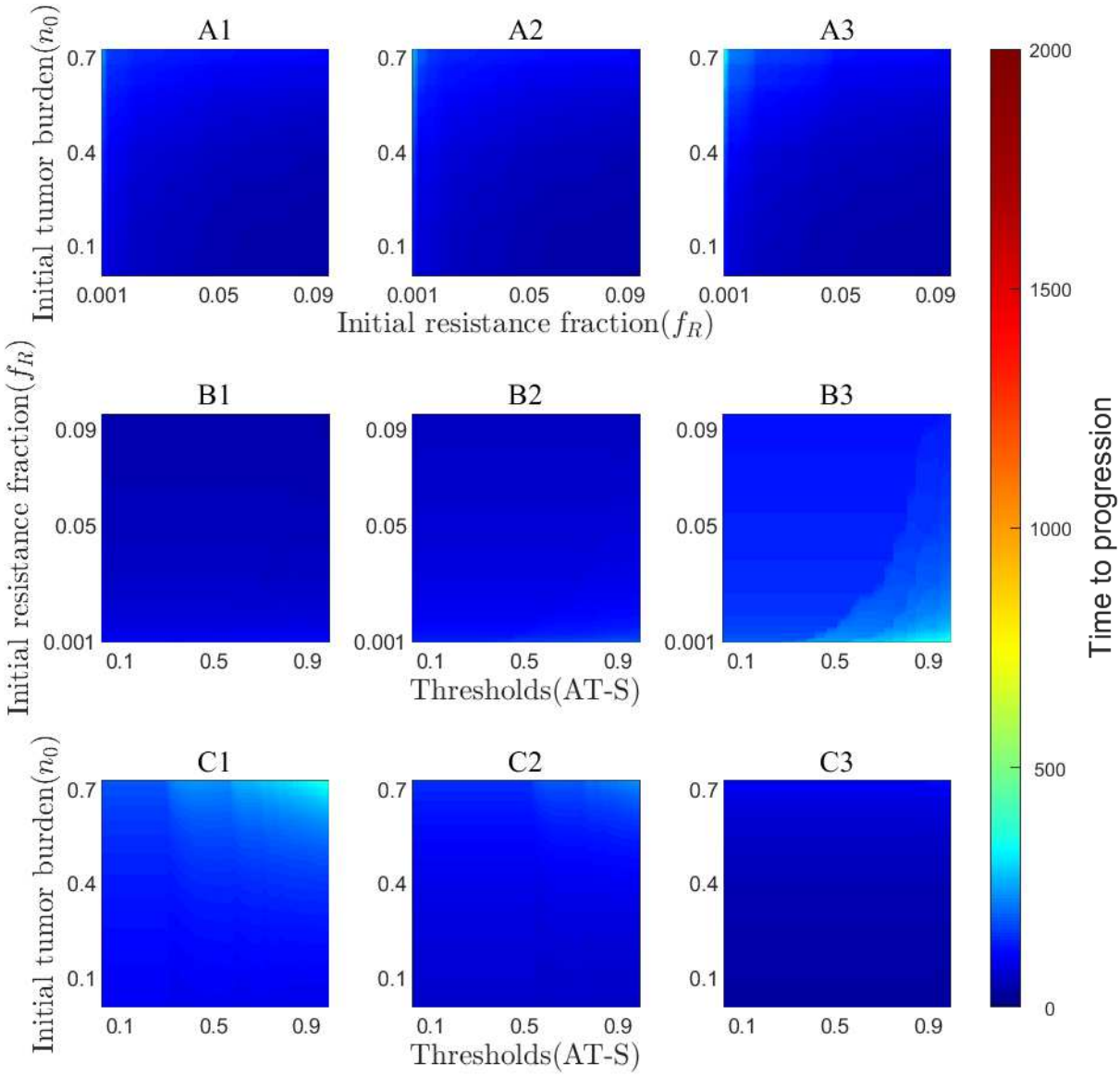

FIGURE S6. The dependence of TTP on the thresholds, initial tumour burden (n_0) and initial fraction of resistant cells (f_R) in neutral competition with $r_S/r_R = 0.6019$, $r_S = 0.0445$. **(A1)-(A3)** Effects of varying initial resistance proportions and tumour burdens on TTP, A1: $C_{\mathrm{TH0}} = 0.3$; A2: $C_{\mathrm{TH0}} = 0.5$; A3: $C_{\mathrm{TH0}} = 0.8$ **(B1)-(B3)** Effects of varying treatment-holiday thresholds and initial resistance proportions on TTP. B1: $n_0 = 0.25$; B2: $n_0 = 0.5$; B3: $n_0 = 0.75$ **(C1)-(C3)** Effects of varying treatment-holiday thresholds and initial tumour burden on TTP, C1: $f_R = 0.001$; C2: $f_R = 0.01$; C3: $f_R = 0.1$.

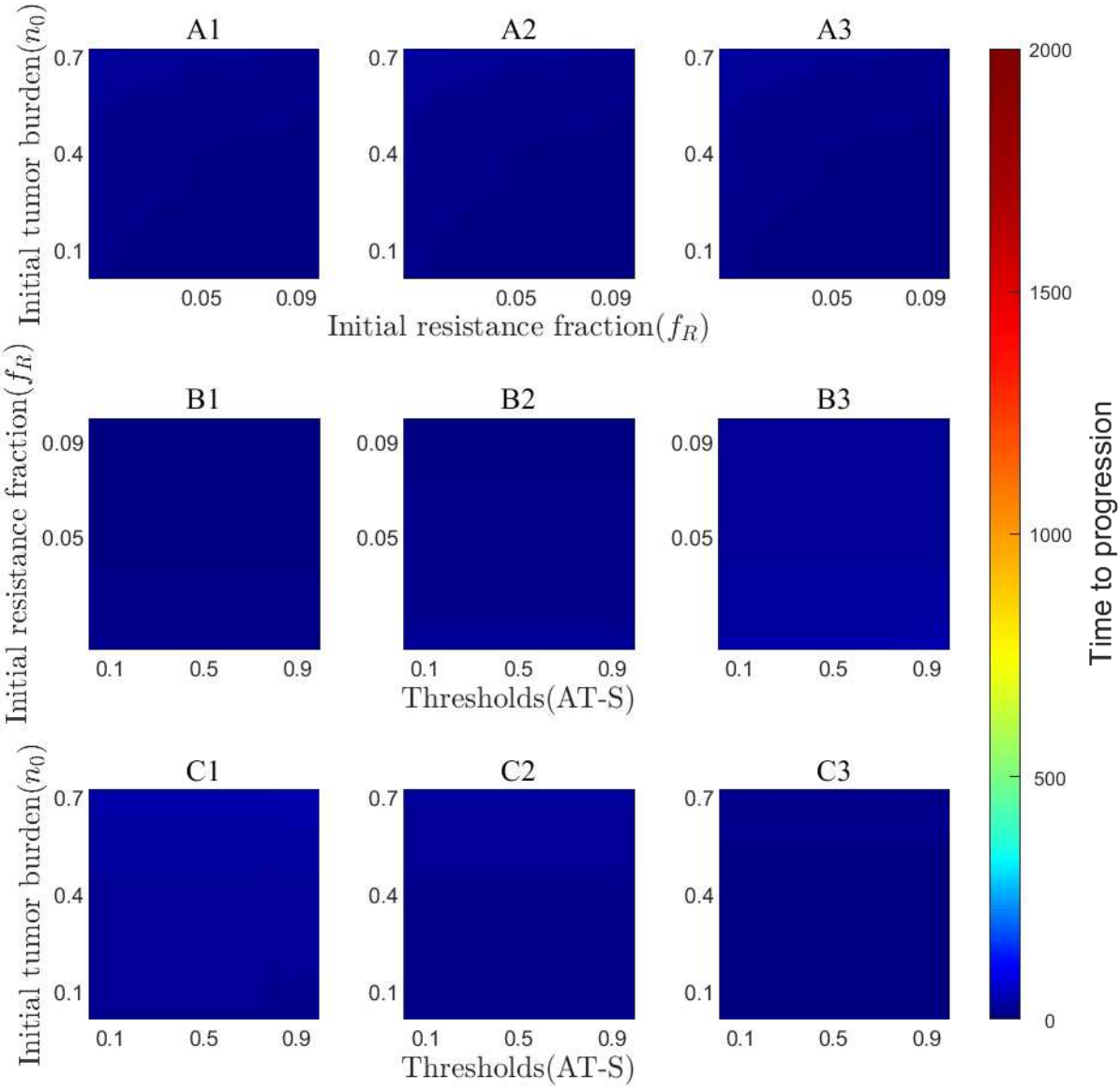

FIGURE S7. The dependence of TTP on the thresholds, initial tumour burden (n_0) and initial fraction of resistant cells (f_R) in neutral competition with $r_S/r_R = 0.1228$, $r_S = 0.0695$. **(A1)-(A3)** Effects of varying initial resistance proportions and tumour burdens on TTP, A1: $C_{\mathrm{TH0}} = 0.3$; A2: $C_{\mathrm{TH0}} = 0.5$; A3: $C_{\mathrm{TH0}} = 0.8$ **(B1)-(B3)** Effects of varying treatment-holiday thresholds and initial resistance proportions on TTP. B1: $n_0 = 0.25$; B2: $n_0 = 0.5$; B3: $n_0 = 0.75$ **(C1)-(C3)** Effects of varying treatment-holiday thresholds and initial tumour burden on TTP, C1: $f_R = 0.001$; C2: $f_R = 0.01$; C3: $f_R = 0.1$.

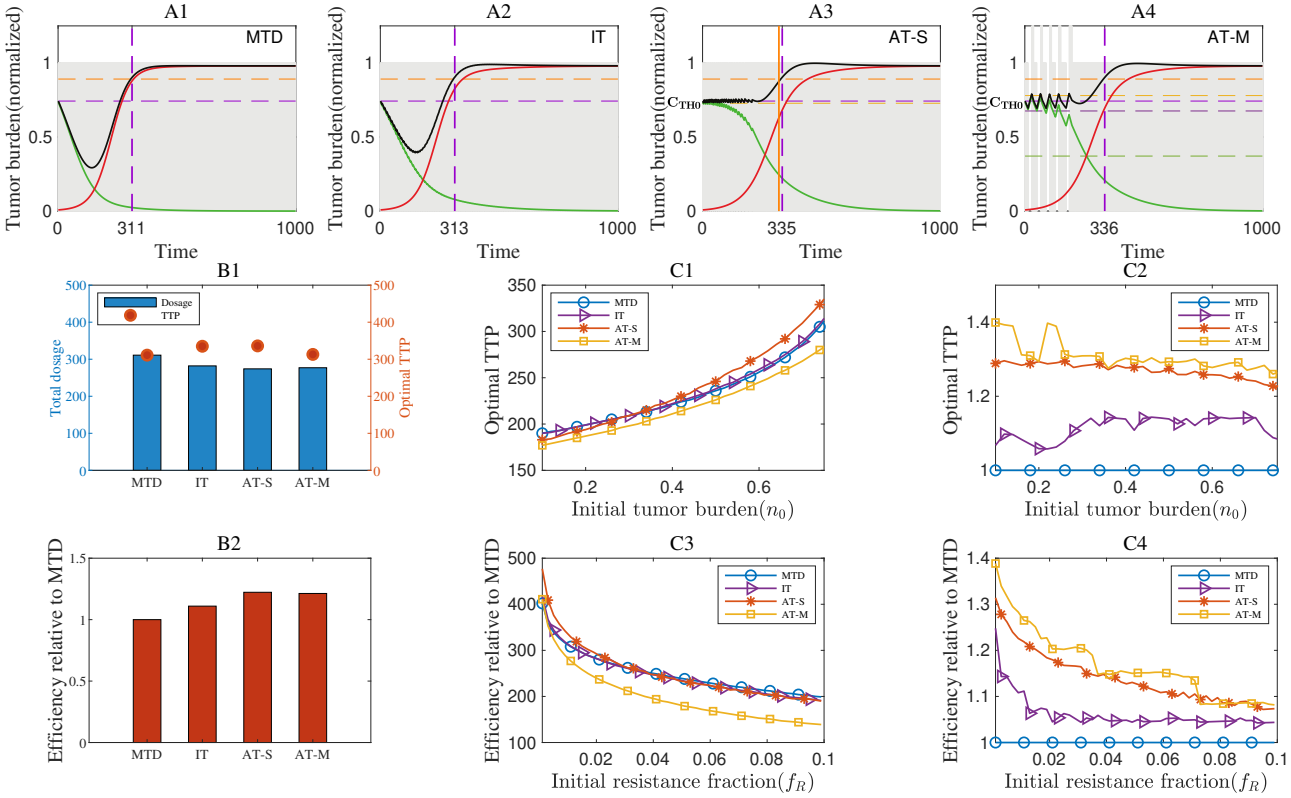

FIGURE S8. Comparison of four treatment strategies on TTP in the scenario of **conditional-improve** where the parameters are taken as $\alpha = 0.6$,$\beta = 0.5$, $f_R = 0.01$ and $n_0 = 0.75$. **(A1)-(A4)** tumour dynamics under four treatment strategies with optimal treatment parameters. Adaptive therapy outperforms MTD and IT. Optimal treatment parameters: $C_{\mathrm{TH0}} = 0.98$ as shown in orange dashed lines which is very close to the purple lines, $\delta_1 = 0.25$, $\delta_2 = 0.25$, $C_{\mathrm{TH2}} = 1.05$ and $C_{\mathrm{TH1}} = 1.07$, $T_D = 9$, $T = 10$. **(B1)** Cumulative drug toxicity (total dosage) and corresponding TTP for the four strategies. **(B2)** Relative efficiency for the four strategies. **(C1)-(C2)** Effects of varying the initial tumour cell proportion on TTP and Relative efficiency of the four strategies. **(C3)-(C4)** Effects of varying the initial resistant cell proportion on TTP and Relative efficiency of the four strategies.

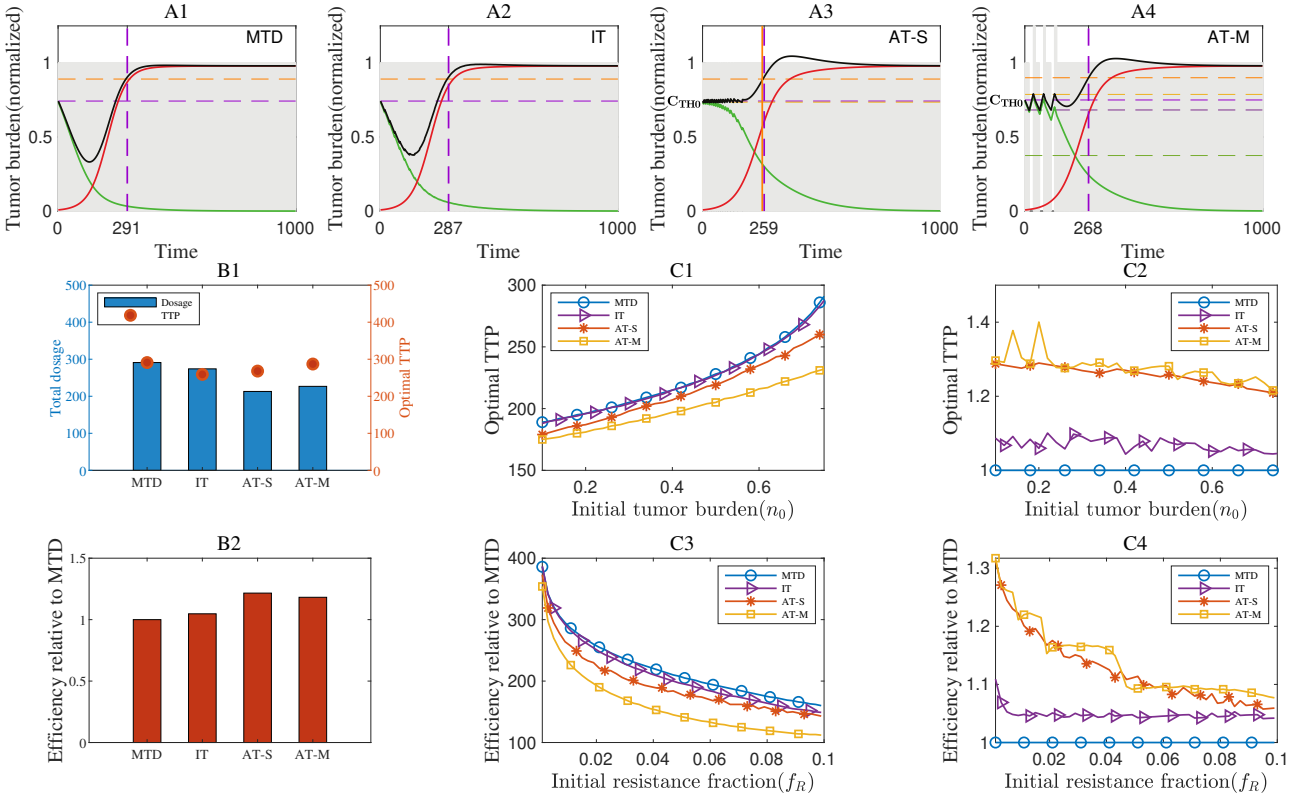

FIGURE S9. Comparison of four treatment strategies on TTP in the scenario of **uniform-improve** scenario where the parameters are taken as $\alpha = 0.6$, $\beta = 0.3$, $f_R = 0.01$ and $n_0 = 0.75$. **(A1)-(A4)** tumour dynamics of tumour evolution with four treatment strategies with optimal treatment parameters. Optimal parameters are taken as follows. $C_{\mathrm{TH0}} = 0.98$ as shown in orange dashed lines which is very close to the purple lines, $\delta_1 = 0.25$, $\delta_2 = 0.25$, $C_{\mathrm{TH2}} = 1.05$ and $C_{\mathrm{TH1}} = 1.09$, $T_D = 20$, $T = 21$. **(B1)** Cumulative drug toxicity (total dosage) and corresponding TTP for the four strategies. **(B2)** Relative efficiency for the four strategies. **(C1)-(C2)** Effects of varying the initial tumour cell proportion on TTP and Relative efficiency of the four strategies. **(C3)-(C4)** Effects of varying the initial resistant cell proportion on TTP and Relative efficiency of the four strategies.

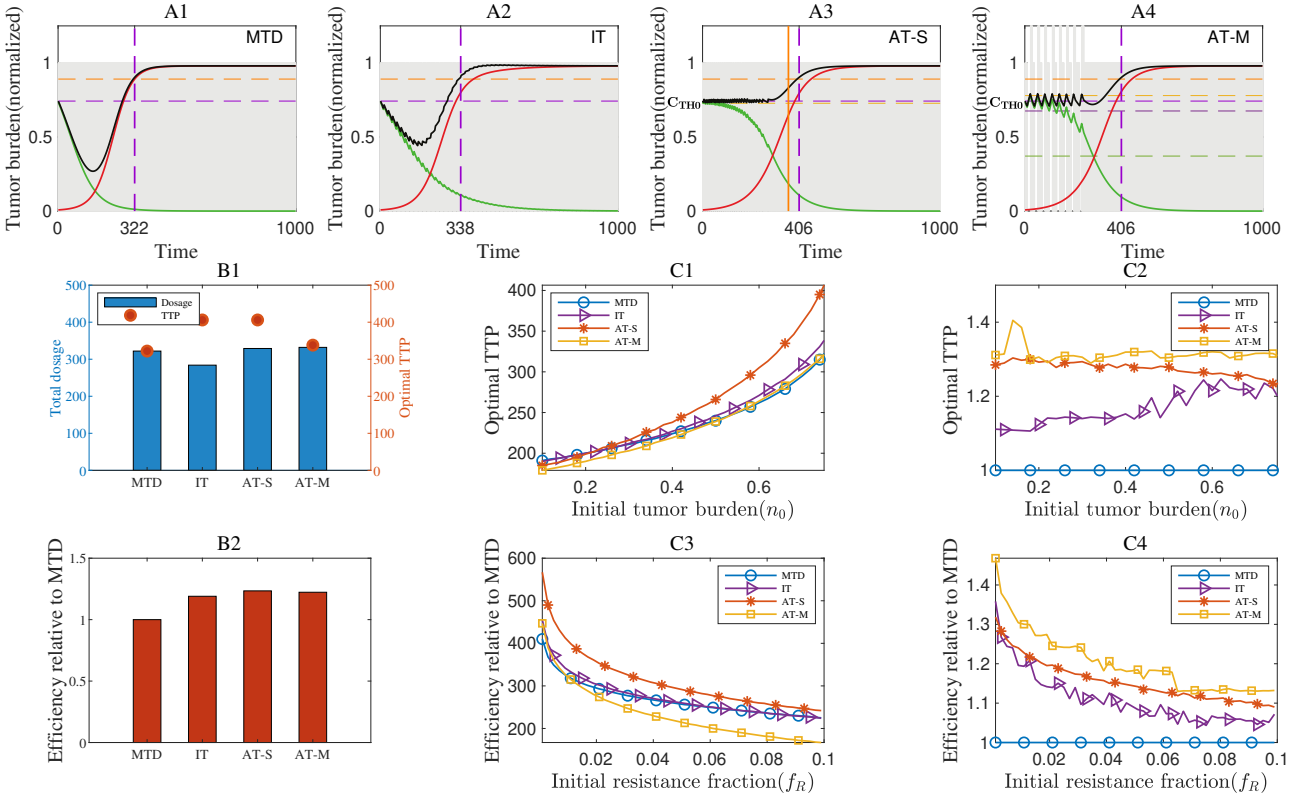

FIGURE S10. Comparison of four treatment strategies on TTP in the scenario of **uniform-decline** where the parameters are taken as $\alpha = 0.3$, $\beta = 0.6$, $f_R = 0.01$ and $n_0 = 0.75$) **(A1)-(A4)** tumour dynamics under four treatment strategies with optimal treatment parameters. Optimal parameters are as follows. $C_{\mathrm{TH0}} = 0.98$ as shown in orange dashed lines which is very close to the purple lines, $\delta_1 = 0.25$, $\delta_2 = 0.25$, $C_{\mathrm{TH2}} = 1.05$ and $C_{\mathrm{TH1}} = 1.05$, $T_D = 15$, $T = 18$. **(B1)** Cumulative drug toxicity (total dosage) and corresponding TTP for the four strategies. **(B2)** Relative efficiency for the four strategies. **(C1)-(C2)** Effects of varying the initial tumour cell proportion on TTP and Relative efficiency of the four strategies. **(C3)-(C4)** Effects of varying the initial resistant cell proportion on TTP and Relative efficiency of the four strategies.

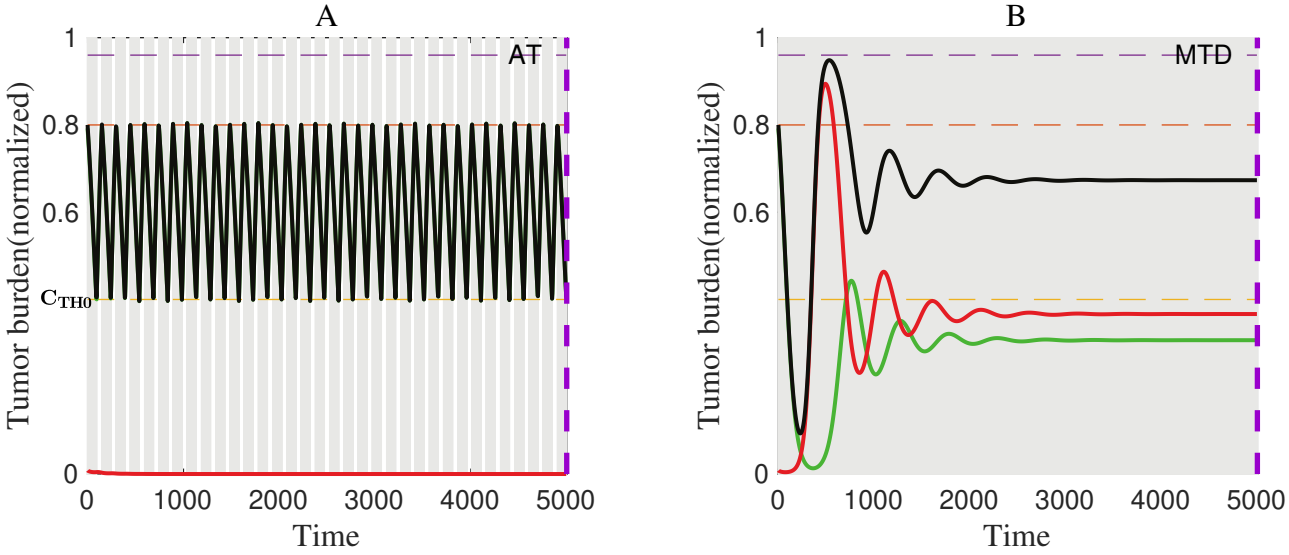

FIGURE S11. tumour evolution dynamics with $\alpha = 2$, $\beta = 2$. Purple dashed line: TTP; Red: Resistant cells; Green: Sensitive cells; Black: Total tumour burden; Shaded area: Treatment implementation. **(A)** Adaptive therapy ($n_0 = 0.8$, $f_R = 0.01$, $C_{\mathrm{TH0}} = 0.5$). **(B)** Maximum tolerated dose ($n_0 = 0.8$, $f_R = 0.01$).

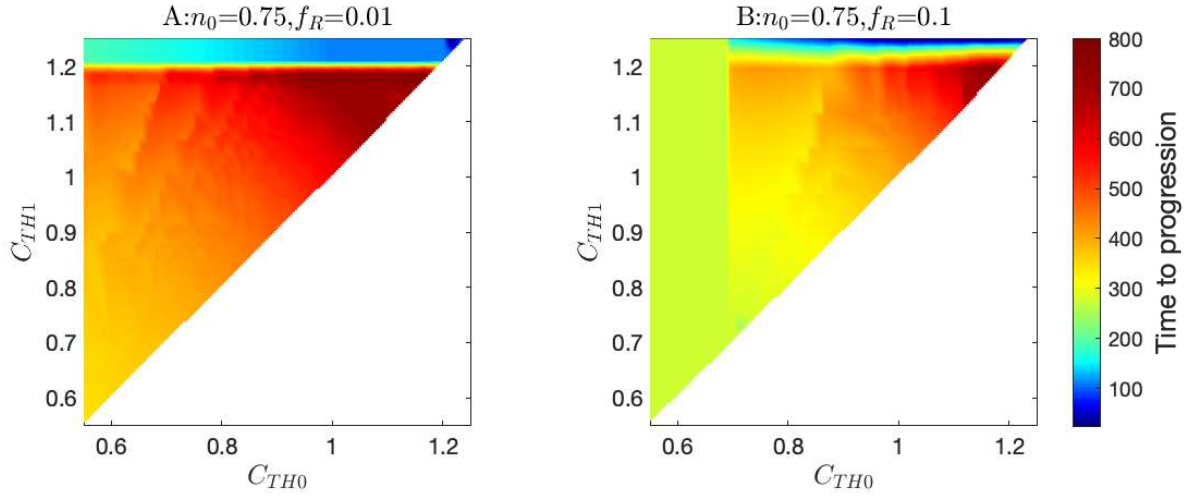

FIGURE S12. Dependence of TTP on the two thresholds C_{TH0} and C_{TH1}. The blue regions in the upper parts of the figures correspond to scenarios where TTP is inferior to that achieved with MTD. This occurs because C_{TH1} exceeds the limits of progression which prevents therapy from restarting before progression is reached. **(A)** The impacts of simultaneous changing C_{TH0} and C_{TH1} on TTP, given the initial tumour burden $n_0 = 0.75$ and the initial resistant cell fraction $f_R = 0.01$. **(B)** The impacts of simultaneous changing C_{TH0} and C_{TH1} on TTP, given $n_0 = 0.75$ and $f_R = 0.1$.

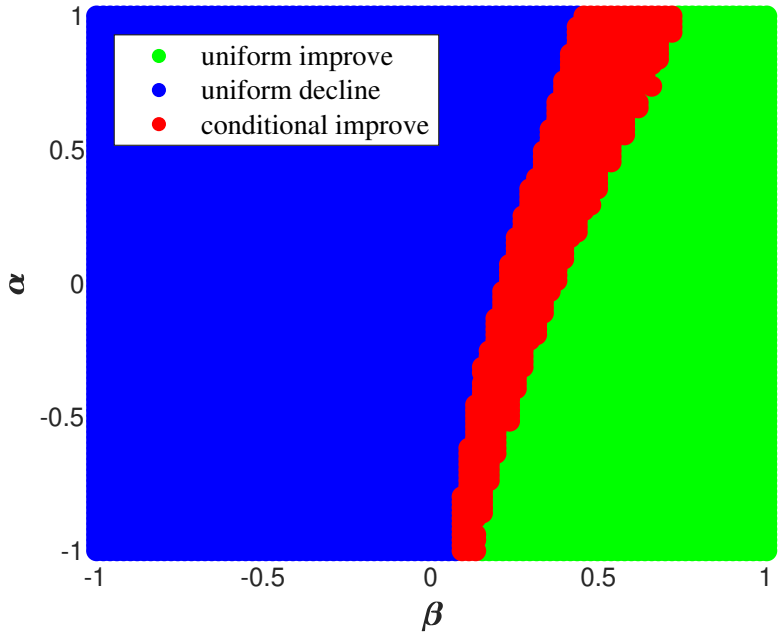

FIGURE S13. Dependence of the three scenarios on the competition coefficients, with the initial tumour burden $n_0 = 0.75$, the fraction of resistant cells $f_R = 0.01$, and other parameters set as in Table 1. Here only the treatment-holiday threshold C_{TH0} varies.

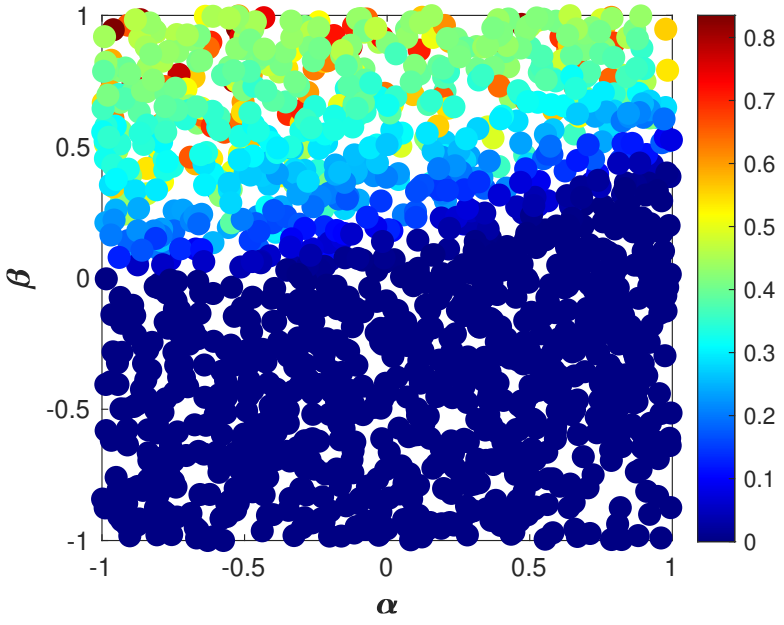

FIGURE S14. Dependence of the probability of selecting adaptive therapy on competition coefficients. The color indicates the probability of selecting adaptive therapy, that is, the condition where the TTP of adaptive therapy is better than MTD. Here, the initial fraction of resistant cells f_R, cell division rates r_S and r_R, and treatment-holiday thresholds C_{TH0} and C_{TH1} are randomly sampled to represent various individual conditions. The sample size is 1500 for each pair of competition coefficient values α and β.

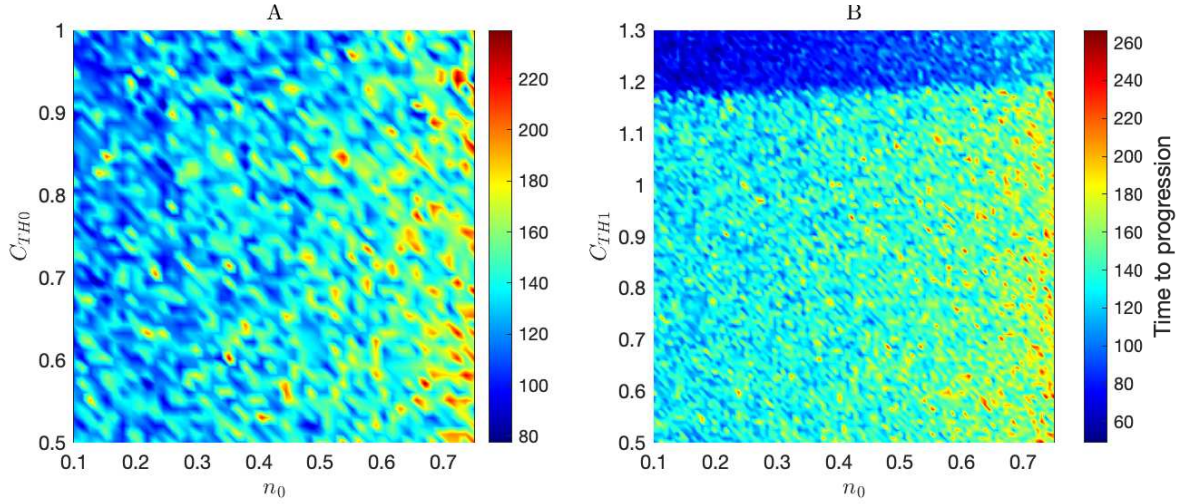

FIGURE S15. Dependence of TTP on the initial conditions and two thresholds with α and β ranging in $(-1, 1)$. The parameters other than those indicated in the axes are chosen randomly within certain ranges to represent various individual conditions, including the fraction of resistant cells f_R, cell division rates r_S and r_R, and treatment-holiday thresholds C_{TH0} and C_{TH1}. The sample size is 1500 for each pair of the parameters indicated in the axes.